ISSN 2744-2640
e-ISSN 2744-2659
JST&M, Vol. 3
www.mtf.unze.ba
04

Journal of **Sustainable Technologies and Materials**

Zenica, June 2023

Journal of Sustainable Technologies and Materials (ISSN 2744-2640)
Vol. 3, No. 4(2022), 1 – 48

Published by
The University of Zenica, Faculty of Metallurgy and Technology

Editorial office
Travnička cesta 1,72000 Zenica
Bosnia and Herzegovina
Phone: +387 32 403 468
Email: jstm@unze.ba
Website: https://www.mtf.unze.ba

Editor-in-Chief
Farzet Bikić, The University of Zenica, Faculty of Metallurgy and Technology, B&H

Associate Editors
Hasan Avdušinović, B&H, University of Zenica, Faculty of Metallurgy and Technology
Ilhan Bušatlić, B&H, University of Zenica, Faculty of Metallurgy and Technology
Diana Ćubela, B&H, University of Zenica, Faculty of Metallurgy and Technology
Jusuf Duraković, B&H, University of Zenica, Faculty of Metallurgy and Technology
Almaida Gigović-Gekić, B&H, University of Zenica, Faculty of Metallurgy and Technology
Adnan Mujkanović, B&H, University of Zenica, Faculty of Metallurgy and Technology

Editorial Board Members
Elvis Ahmetović, B&H, University of Tuzla, Faculty of Technology,
Ljubiša Balanović, Serbia, University of Belgrade, Technical Faculty Bor,
Mirjana Čurlin, Croatia, University of Zagreb, Faculty of Food Technology and Biotechnology
Sead Ćatić, B&H, University of Tuzla, Faculty of Technology
Kemal Delijić, Montenegro, University of Montenegro, Faculty of Metallurgy and Technology,
Natalija Dolić, Croatia, University of Zagreb, Faculty of Metallurgy Sisak,
Mirko Gojić, Croatia, University of Zagreb, Faculty of Metallurgy Sisak
Nenad Gubeljak, Slovenia,
The University of Maribor, Faculty of Mechanical Engineering,
Safija Herenda, B&H, University of Sarajevo, Faculty of Science
Nusret Imamović, B&H, University of Zenica, Faculty of Mechanical Engineering
Fehim Korać, B&H, University of Sarajevo, Faculty of Sciences
Borut Kosec, Slovenia, University of Ljubljana, Faculty of Natural Sciences and Engineering
Tibela Landeka Dragičević, Croatia, University of Zagreb, Faculty of Food Technology and Biotechnology
Dragan Manasijević, Serbia, University of Belgrade, Technical Faculty Bor
Sanja Martinović, Serbia, University of Belgrade, Faculty of Technology and Metallurgy
Viorica Musat, Romania, "Dunărea de Jos" University of Galati, **Aleš Nagode**, Slovenia, University of Ljubljana, Faculty of Natural Sciences and Engineering.
Vesna Ocelić Bulatović, Croatia, University of Zagreb, Faculty of Metallurgy Sisak
Iulian Riposan, Romania, University Politehnica of Bucharest, Materials Science and Engineering Faculty
Luca Sportelli, New Zealand, St. Clements University, Niue,
Aida Šapčanin, B&H, University of Sarajevo, Faculty of Pharmacy
Nada Štrbac, Serbia, University of Belgrade, Technical Faculty Bor
Anita Štrkalj, Croatia, University of Zagreb, Faculty of Metallurgy Sisak,
Iveta Vaskova, Slovakia, Technical University of Košice, Faculty of Materials, Metallurgy and Recycling,
Asim Vehbi, North Cyprus,
Arkin University of Creative Arts and Design (ARUCAD)
Milica Vlahović, Serbia, University of Belgrade, Faculty of Technology and Metallurgy,
Tatjana Volkov-Husović, Serbia, University of Belgrade, Faculty of Technology and Metallurgy,
Zdenka Zovko Brodarac, Croatia, University of Zagreb, Faculty of Metallurgy Sisak,

English Language Editor
Hasan Avdušinović, University of Zenica, Faculty of Metallurgy and Technology, B&H
Diana Ćubela, University of Zenica, Faculty of Metallurgy and Technology, B&H

For submission instructions, manuscript submission, and additional information, please visit https://www.mtf.unze.ba/.

Disclaimer: The Publisher and Editors cannot be held responsible for errors or any consequences arising from the use of the information contained in this journal. The views and opinions expressed do not necessarily reflect those of the Publisher and Editors, and neither does the publication of advertisements constitute any endorsement by the Publisher and Editors of the product advertised.

Computer design
Safet Hamedović, University of Zenica, Faculty of Metallurgy and Technology

Cover design:
Admir Velić

Printed by „Štamparija Fojnica" D.D. Fojnica, B&H, in June 2023

CONTENTS

1. ***Influence of current density on leachate treatment efficiency by electrocoagulation with zeolite addition*** *1*
   Nediljka Vukojević Medvidović, Ladislav Vrsalović, Sandra Svilović, Mirjana Cestarić

2. ***Removal of heavy metals from landfill leach water using pyrophyllite as adsorbent*** *7*
   Jasmina Kustura, Belma Halilhodžić, Enita Kurtanović, Amra Čizmić, Kenan Kozlo, Adnan Teletović, Atif Hodžić, Muhamed Harbinja

3. ***Analysis of production method and stabilizing agent on structure of aluminum metal foams*** *16*
   Karla Grgić, Igor Ćulum, Branimir Lela, Jure Krolo, Sonja Jozić

4. ***Effect of particle shape and size of copper powders on the properties of sintered parts*** *22*
   Ivana Marković, Dragan Manasijević, Ljubiša Balanović, Uroš Stamenković, Milijana Mitrović, Stevan Trujić

5. ***Effect of addition of wet-strength agent on tensile strength of paper*** *30*
   Edina Husić, Šefkija Botonjić

6. ***Polymeric materials in gluing techniques*** *36*
   Šaćira Mandal, Aida Šapčanin

JST&M 4(2023), 1 - 6
DOI: 10.57131/jstm.2023.4.1

Original scientific paper

INFLUENCE OF CURRENT DENSITY ON LEACHATE TREATMENT EFFICIENCY BY ELECTROCOAGULATION WITH ZEOLITE ADDITION

Nediljka Vukojević Medvidović, Ladislav Vrsalović, Sandra Svilović and Mirjana Cestarić

University of Split, Faculty of Chemistry and Technology

ABSTRACT

The electrocoagulation with zeolite addition was used to treat compost leachate. The effects of different current densities and zeolite particle sizes on electrode dissolution, electrode surface condition, and removal efficiency were investigated. The surface of the electrodes was analysed by optical microscope, while the consumption of the aluminium electrodes was investigated by weighing. The results confirmed that the removal efficiency could be improved by conducting the experiment at higher current densities, but the electrodes used were significantly more damaged. Significant damage was also observed on the electrode used in the experiment with larger zeolite particles, which can be related to the stronger abrasion effect.

Keywords: current density, electrode surface, aluminium

Corresponding Author:
Nediljka Vukojević Medvidović
Faculty of Chemistry and Technology in Split
Ruđer Bošković 35, 21000 Split, Croatia
Tel.: + 385 21 329 452; fax: + 385 21 329 461
E-mail address: nvukojev@ktf-split.hr

1. INTRODUCTION

Electrocoagulation (EC) is a process that combines coagulation, flocculation, flotation, and electrochemical anodic and cathodic reactions to remove pollutants from wastewater. It is based on the formation of flocs of metal hydroxides by dissolving the electrodes, which serve as flocculants on which pollutants can be removed by the *sweep flock* mechanism [1-7]. In general, the electrochemical reactions taking place in an EC reactor with immersed metal electrodes (M), and with aluminium electrode can be represented by the following equations [2,8]:

anode

$$Al_{(s)} \rightarrow Al^{3+}_{(aq)} + 3e^- \quad (1)$$

$$2H_2O_{(l)} \rightarrow 4H^+_{(aq)} + O_2(g) + 4e^- \quad (2)$$

cathode

$$2H_2O_{(l)} + 2e^- \rightarrow 2H_{2(g)} + OH^- \quad (3)$$

$$2O_{2(g)} + 4H^+ + 4e^- \rightarrow 2H_2O \quad (4)$$

Oxidation of the aluminium occurs at the anode, causing the aluminium anode to dissolve (or corrode) and produces aluminium metal cations that instantly undergo further reactions to form different metal (oxy) hydroxides. At the same time, an anodic oxygen evolution reaction (OER) takes place (reaction 2), so there is competition between aluminium dissolution and OER. According to Tegladza et al. [2], at low current density, aluminium dissolution mainly occurs, while at high current density, both processes compete. At the cathode, a hydrogen evolution reaction (HER) occurs (reaction 3), while under the condition of high dissolved oxygen content, an oxygen reduction reaction (ORR) also takes place (reaction 4) [2,8].

Corrosion product formation reaction of $Al(OH)_3$ which serves as flocculants is given by equation (5). Namely, the Al^{3+} ions generated at the anode and OH^- produced at the cathode undergo several speciation reactions and generate intermediate species (such as $Al(OH)^{2+}$, $Al_2(OH)_2^{4+}, Al_7(OH)_{17}^{4+}$, $Al_{13}O_4(OH)_{24}^{7+}$, which are the precursors to the formation of the stable insoluble $Al(OH)_3$ flocs [8].

$$Al^{3+}_{(aq)} + 3OH^- \rightarrow Al(OH)_{3(s)} \tag{5}$$

During EC processes, the appearance of passivation on the metal surface of the electrode causes an increase in potential [2]. Thus, passivation can reduce the dissolution process of metal cations from the electrodes and leads to increased electricity consumption. To prevent the occurrence of passivation, the addition of specific anions in the solution (so-called activators, like chloride ions), regular mechanical cleaning, and rinsing of the electrode surface or electrode polarity change are usually used [2, 9-12]. Therefore, further research is needed to provide a new solution that can contribute to better electrode dissolution. Our previous researches confirm that the zeolite addition in the EC process may enhance the EC treatment efficiency [13-16]. Moreover, the abrasive effect of zeolite particles on the electrode surface was also recorded, which can reduce the passivation effect.

The purpose of this paper is to investigate how changing the parameters of the EC experiments, such as different sizes of zeolite particles and different current densities, will affect the change in the surface of aluminium electrodes during the EC experiment, electrode consumption, and removal efficiency. The surfaces of the electrodes were analysed by optical microscope, while the consumption of the aluminium electrodes was investigated by weighing method. Treatment efficiency was evaluated by measuring pH, temperature, total solids, COD, and turbidity.

2. EXPERIMENT

2.1 Materials

Compost leachate was collected during the composting of biowaste in the "C-EcoForHome" composter with the use of "Compost Help" anaerobic microorganisms. Compost leachate is characterized by acidic pH (pH=4.03), very high organic load (initial COD equals 10427.6 mg O_2/L), very high electrical conductivity of 3.54 mS/cm, turbidity of 397 NTU, and total solids (TS) of 10.33 g/L. All measured parameters are determined according to the Standard Water and Wastewater Testing Methods [17].

Electrode material: The aluminum alloy AA 2007 series 2000 was used as electrodes (anode and cathode), in which the main alloying element is copper (Al=92.58%, Cu=3.84%).

Synthetic zeolite: The synthetic zeolite NaX was purchased from Sigma-Aldrich (zeolite type with $r_{Si/Al}$ = 1.23). Before use, the zeolite was crushed and sieved into two different granulations of NaX particles of 160-600 µm and < 90 µm.

2.2 Performance of the electrocoagulation process

Electrocoagulation (EC) was carried out in a 350 mL of electrochemical cell, with immersed aluminum electrodes and with the addition of 20 g/L NaX zeolite (particle zeolite size of <90 µm or 160-600 µm), without the addition of electrolyte. The initial pH of the solution was 4.03. Distance between electrodes was maintained at 3 cm and a mixing speed of 100 rpm and the working EC time was 30 min. The applied current density values were i = 0.018 A/cm^2 and 0.009 A/cm^2. Experiments labelling and working conditions are summarized in Table 1.

Table 1. Experiments labelling and working conditions

Experiments labelling	Working conditions Al electrode, t = 30 min, electrode distance = 3 cm, mixing speed =100 rpm
A1	EC, NaX (< 90 µm), i=0.009 A/cm^2
A2	EC, NaX (< 90 µm), i=0.018 A/cm^2
A3	EC, NaX (160-600 µm), i=0.009 A/cm^2
A4	EC, NaX (160-600 µm), i=0.018 A/cm^2

For each EC process, pH, temperature, total solids, turbidity, and COD were measured according to Standard Methods of Water and Wastewater Analysis [17].

2.3 Electrode surface preparation and consumption loss analysis

Before each measurement, the surfaces of the Al electrodes were ground with P240, P400, P600, and P800 grit water-based abrasive papers using Metkon Forcipol 1V metallographic grinding and polishing machine manufactured by Metkon, Turkey. After mechanical processing, the electrodes were ultrasonically degreased in ethanol, washed in deionized water, dried, and weighed on an analytical balance before use. The electrode consumption was determined by weighing both electrodes (anode and cathode) on analytical balance before and after each experiment.

2.4 Examination of the electrode surface with a light microscope

The electrode surface of the aluminum electrodes (anode and cathode) after the EC process was examined with a light microscope MXFMS-BD, Ningbo Sunny Instruments Co. with a magnification of 100 times. The is a trinocular microscope on which a Canon EOS 1300D digital camera is mounted and used to photograph the surface of the samples. The microscope is connected to the computer via a camera, and the image of the surface is projected on the computer monitor.

3. RESULTS AND DISCUSSION

3.1 Analysis of the electrode surface before and after the implementation of the electrocoagulation process using a light microscope

Electrochemical processes at the anode and cathode, as well as exposure of the electrodes to leachate produced by anaerobic composting, lead to significant changes on the surface of the electrodes. For this reason, it is important to examine the condition of the surface of the electrodes after carrying out the process in order to determine the degree of wear and the form of corrosion attack on the electrodes. Therefore, the surfaces of the anodes and cathodes, before and after the implementation of the electrocoagulation process, were recorded using a light microscope with a magnification of 100 times and comparisons are given in Figure 1.

Despite the fact that polished Al alloy electrodes are shiny and smooth (image on the left side of Figure 1), microscopic pictures reveal surface inhomogeneity. Microscopic images of the electrodes after mechanical processing by grinding and before the EC process (image on the left side of Figure 1) show sandpaper "lines" which are clearly visible. The surface's small residual roughness aids in the dissolution of the electrodes, which is helpful in this situation, and no additional polishing is needed. Namely, the main alloying element of the 2000 series alloys is Cu, which improves the mechanical properties of the alloys of this series, but at the same time worsens their corrosion properties. Consequently, such alloys have significantly lower corrosion resistance compared to pure Al.

The image for anodes and cathodes on the right side of Figure 1 shows the appearance of the electrodes after the EC process. After each experiment, the anode and cathode lost their shine and smoothness, and damage and "roughness" of the surface caused by corrosion processes are visible. The surfaces of the anodes are significantly corroded due to the intensive dissolution process, whereby two dominant forms of corrosion are visible: general and pitting corrosion. Dots on the cathodes indicate the occurrence of pitting corrosion. The amount and size of the dots depend on the experimental conditions. In addition to dots, cracked surfaces are also present, indicating the existence of a layer of corrosion products.

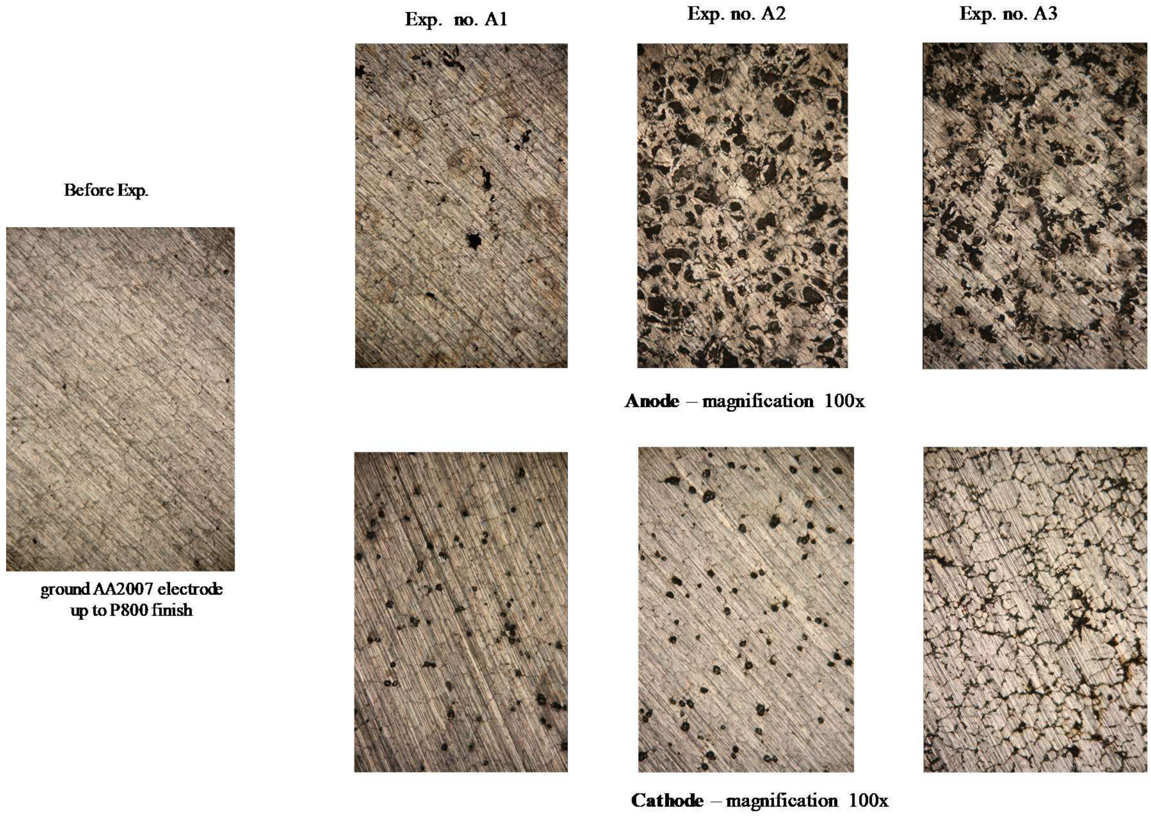

Figure 1. Comparison of Al electrode surface before and after EC process at experimental conditions of A1, A2, and A3

Comparing the surface of the electrodes after process A1 (with a current density of 0.009 A/cm^2) and A2 (with a current density of 0.018 A/cm^2), significantly greater damage is visible on the electrodes with higher values of current density. The difference in the surface appearance of the electrodes in experiment A1, in which zeolite with smaller particle sizes was used, and in experiment A3, in which zeolite with larger particle sizes was used, is also visible. The electrodes, used for experiment A3, were significantly damaged, which can be connected to the stronger abrasive effect of larger zeolite particles.

3.2 Electrode consumption analysis

Electrode consumption was determined during each experiment by weighing the anode and cathode before and after the EC process and the results are presented in Figure 2.

High anode consumption is observed in all EC experiments, but cathode consumption was also evident. Regarding the influence of current densities, higher anode consumption was observed in experiments with higher current densities of 0.018 A/cm^2, while at lower values of the current density of 0.009 A/cm^2, the cathode consumption was higher. The impact of zeolite particle size was almost insignificant for lower current density (experiment A1/A3). However, at a higher current density, particle size affects cathode and anode consumption (experiment A2/A4).

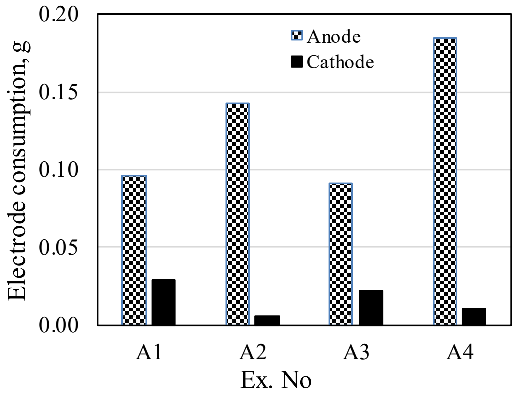

Figure 2. Comparison of anode and cathode electrode consumption

The corrosion of the anode was expected, however, the corrosion of the cathode confirms the occurrence of a different mechanism of electrode dissolution in the EC process, which is characteristic of Al electrodes [13-16].

3.3 Efficiency analysis

During each EC experiment, the pH, temperature, total solids, and COD were determined and the results are summarised in Table 2.

Table 2. Results of pH in final solutions, initial and final temperature values, the total solids, turbidity, and COD for each EC experiment

Exp. no.	Experiment mark	pH_{fin}, -	T_{in}, °C	T_{fin}, °C	TS, g/L	Turbidity decrease, %	COD decrease, %
A1	EC-NaX (< 90 µm), i=0.009 A/cm^2	6.76	23.2	28.9	11.45	87.88	17.56
A2	EC-NaX (< 90 µm), i=0.018 A/cm^2	7.14	22.8	34.1	11.99	70.28	32.82
A3	EC- NaX (160-600 µm), i=0.009 A/cm^2	5.76	22.8	29.6	11.03	88.94	31.30
A4	EC-NaX (160-600 µm), i=0.018 A/cm^2	5.83	23.5	41.6	10.19	97.00	51.91

An increase of initial pH values from 4.03 to pH in the range of 5.76-7.14 is evident in all experiments, which is mainly associated with the formation of OH^- ions at the cathode (reaction 3) [2]. The slightly higher increase is observed with a smaller zeolite particle site of < 90 µm (pH is in the range of 6.76-7.14), compared to the larger zeolite particle size (pH is in the range of 5.76-5.83). Also, higher current density values result in a slightly higher increase in pH values. Even a rise in pH is observed in all experiments, this rise is lower than it is expected according to literature (pH ≈8) [13-16], which can be attributed to the complex composition of the initial compost leachate solution, which practically acts like a buffer. During each experiment, a significant increase in temperature is observed (final temperature is in the range of 28.9-41.6 °C), which is connected with higher electrode consumption (see Figure 2). A similar was observed previously [13-16]. Values of TS oscillate around initial TS values of 10.33 g/L, in dependence on experimental conditions. Namely, the initial TS values are significantly high, and thus no significant reduction was observed in the final solution.

Turbidity and COD decrease was observed. The turbidity decrease was significant (in the range 70.28-97.00 %) compare to the COD decrease (in the range of 17.56-51.91%). The best turbidity and COD removal was observed at experiment A4 (at higher zeolite particle and higher current density). This indicates that larger zeolite particle size and higher current density enhance Al electrode dissolution and formation of Al flock, thus removal of a higher amount of soluble and colloidal species from compost leachate is observed.

Even significant turbidity reduction was achieved with the application of the EC process, final values of COD in all experiments significantly exceed the limit values prescribed by Croatian regulation for discharge into natural surface water and public sewage system (125 mg O_2/L) [18], thus additional treatment process needs to be performed before final discharge.

4. CONCLUSION

Microscopic images of the electrodes after the electrocoagulation process indicate significant damage to the electrode surface. The surfaces of the anodes were severely corroded due to the intense dissolution process, with general and pitting corrosion observed. The appearance of pitting corrosion is visible on the cathodes, along with the presence of a cracked surface indicates the existence of a layer of corrosion products. Increased values of current density induced higher electrode damage. Also, significant damage was observed on the electrode that was used in the experiment with larger zeolite particles, which can be associated with its stronger abrasive effect. Anode consumption was more pronounced at higher values of current density and higher zeolite particle size, with the highest turbidity and COD decrease observed.

Conflict of interest

The authors declare that they have no competing interests.

5. References

[1] S. Sen, A. K. Prajapati, A. Bannatwala, D. Pal, Electrocoagulation treatment of industrial wastewater including textile dyeing effluent – a review, *Desalination Water Treat.*, 161(2019), p. 21–34, doi: 10.5004/dwt.2019.24302

[2] I. D. Tegladza, Q. Xu, K. Xu, G. Lv, J. Lu, Electrocoagulation processes: a general review about the role of electro-generated floc in pollutant removal, *Process Saf. Environ. Prot.*, 146(2021), p. 169-189, doi.org/10.1016./j.psep.2020.08.048

[3] I. Kabdaşlı, I. Arslan-Alaton, T. Ölmez-Hancı, O. Tünay, Electrocoagulation applications for industrial wastewaters: a critical review, *Environ. Technol. Rev.,* (2012), p. 1-44, doi.org/10.1080/21622515.2012.715390

[4] D. T. Moussa, M. H. El-Naas, M. Nasser, M. J. Al-Marri, A comprehensive review of electrocoagulation for water treatment: Potentials and challenges, *J. Environ. Manage.,* 186(2017), p. 24–41, doi:10.1016/j.jenvman.2016.10.032

[5] M. Bharath, B. M. Krishna, B. M. Kumar, A Review of electrocoagulation process for wastewater treatment, *Int. J. Chem. Tech. Res.,* 11(2018), p. 289-302, doi.org/10.20902/IJCTR.2018.110333

[6] A. Tahreen, M. S. Jami, F. Ali, Role of electrocoagulation in wastewater treatment: A developmental review, *J. Water Process Eng.*, 37(2020), p. 101440, doi.org/10.1016/j.jwpe.2020. 101440

[7] M. Mousazadeh, E. K. Niaragh, M. Usman, S. U. Khan, M. A. Sandoval, Z. Al-Qodah, Z. B. Khalid, V. Gilhotra, M. M. Emamjomeh, A critical review of state-of-the-art electrocoagulation technique applied to COD-rich industrial wastewaters, *Environ. Sci. Pollut. Res.,* 28(2021), p. 43143–43172, doi.org/10.1007/s11356-021-14631-w

[8] K. S. Hashim, A. Shaw, R. Al Khaddar, M. O.-Pedrola, D. Phipps, Iron removal, energy consumption and operating cost of electrocoagulation of drinking water using a new flow column reactor, *J. Environ. Manage,* 189(2017), p. 98–108, doi:10.1016/j.jenvman.2016.12.035

[9] C. Vargel, *Corrosion of Aluminium*, Elsevier LTd., Netherlands, 2004, p. 96-101

[10] J. Tao, *Surface composition and corrosion behavior of an Al-Cu alloy*, [doctoral thesis], Université Pierre et Marie Curie, Paris VI, 2016, https://tel.archives-ouvertes.fr/tel-01412882

[11] G. Mouedhen, M. Feki, W. De Petris Wery, H. F. Ayedi, Behavior of aluminum electrodes in electrocoagulation process, *J. Hazard. Mater.*, 150 (2008) p. 124–135, doi:10.1016/j.hazmat.2007.04.090

[12] M. Ingelson, N. Yasri, E. P. L. Roberts, Electrode passivation, faradaic efficiency, and performance enhancement strategies in electrocoagulation – a review, *Water Res.,* 180(2020) p. 116433, doi.org./10.1016/j.watres.2020.116433

[13] N. Vukojević Medvidović, L. Vrsalović, T. Brozinčević, S. Svilović, Treatment of municipal wastewater by electrocoagulation and natural zeolite – influence of initial pH values, In: K. Szramowiat-Sala, M. Karczewski, K. Sornek, R. Figaj, (eds.), Book of Abstracts of the 4th International Conference on the Sustainable Energy and Environmental Development, Krakov, Institute of Sustainable Energy, 2021, p. 11

[14] N. Vukojević Medvidović, L. Vrsalović, T. Ugrina, I. Jukić, *Electrocoagulation augmented with natural zeolite—the new hybrid process for treatment of leachate from composting of biowaste*, In: N. Dolić, Z. Zovko Brodarac, S. Brajčinović, (eds.), Proceedings of the 19th International Foundrymen Conference: Humans—Valuable Resource for Foundry Industry Development, Split, Croatia, 16–18 June 2021; Faculty of Metallurgy, University of Zagreb, Zagreb, Croatia, 2021, p. 489–498. https://ifc.simet.hr/?page_id=2518

[15] N. Vukojević Medvidović, L. Vrsalović, S. Svilović, A. Bobanović, Electrocoagulation vs. Integrate Electrocoagulation-Natural Zeolite for Treatment of Biowaste Compost Leachate—Whether the Optimum Is Truly Optimal, *Minerals,* 12(2022), p. 442, doi.org/10.3390/min12040442

[16] S. Svilović, N. Vukojević Medvidović, L. Vrsalović, A. Kulić, Combining Natural Zeolite and Electrocoagulation with Different Electrode Materials – Electrode Surface Analysis and Taguchi Optimization, *App. Surf. Sci. Adv.,* 12(2022), p. 100330, doi.org/10.1016/j.apsadv.2022.100330

[17] A. D. Eaton, L. S. Clesceri, E. W. Rice, A. E. Greenberg, M. A. H. Franson, (eds.), *Standard Methods for the Examination of Water and Wastewater*, 21st ed., American Public Health Association (APHA); American Water Works Association (AWWA); Water Environment Federation (WEF): Washington, DC, USA, 2005

[18] Regulation on emission limit values in wastewater, NN 26/2020 (in Croatian)

JST&M 4(2023), 7 - 15
DOI: 10.57131/jstm.2023.4.2

Original scientific paper

REMOVAL OF HEAVY METALS FROM LANDFILL LEACH WATER USING PYROPHYLLITE AS ADSORBENT

Jasmina Kustura, Belma Halilhodžić, Enita Kurtanović, Amra Čizmić, Kenan Kozlo, Adnan Teletović, Atif Hodžić, Muhamed Harbinja

Innovative Scientific Development Center (INRC), AD Harbi LLC, Sarajevo,

ABSTRACT

Leachate water from sanitary landfills represents one of the most complex global environmental problems. This paper examines the possibility of using aluminosilicate material, pyrophyllite, from the Parsovići deposit, as an adsorbent. It was researched the influence of two granulations of pyrophyllite (0-53 µm and 0-100 µm) on the degree of adsorption of heavy metals (Fe, Ni, Mn) from leachate water from the municipal landfill "Desetine", Tuzla. The adsorption experiment was performed using the Batch method, depending on the contact time between the adsorbent and the adsorbate, the mixing speed, and the mass of the adsorbent, pyrophyllite, through two treatments. The results indicate a higher efficiency of the finer fraction of pyrophyllite, and in the competition of the three examined metals, iron is completely removed in the first treatment with both granulations and then nickel with finer granulation and manganese with coarser. After the first treatment, the unpleasant smell was removed, which is certainly a consequence of the removal of ammonia compounds as the most abundant compounds in leachate water. In these pioneering researches, pyrophyllite proved to be effective, and at the same time, it is a cheap, easily available, and environmentally friendly material for leachate water purification.

Keywords: pyrophyllite Parsovići, adsorption, heavy metals, landfill water

Corresponding Author:
Jasmina Kustura
Innovative Scientific Development Center (INRC), AD Harbi LLC
Tvornička 3, Ilidža, Sarajevo, B&H
Tel.: + 385 33 629 883
E-mail address: info@adharbi.ba

1. INTRODUCTION

Leachate water from sanitary landfills represents highly polluted wastewater and can be defined as all water that has "been in contact" with waste disposed of at the landfill. Leachate landfill water is created by the percolation of precipitation through the layers of disposing of waste, then partly originates from water that is included in the composition of disposing of waste, and partly arises during the process of decomposition of waste [1, 2].

The amount and quality of leachate formed in the body of the landfill depends on the size of the landfill, age, working conditions, biological, chemical, and physical processes at the landfill, climatic conditions at the location, composition, and amount of waste that is disposed of, etc.

Landfill leachate water is mainly loaded with the following pollutants [3]:

- nitrogen compounds in organically bound form or in the form of ammonia,
- compounds with phosphorus,
- heavy metals,
- cations - the most common cations that occur are Na^+, K^+, Mg^{2+}, Ca^{2+},
- anions - Cl^-, SO_4^{2-}, S^{2-} i HCO^{3-},
- organic pollution,
- chlorinated hydrocarbons and pesticides,

- specific organic compounds: aromatic hydrocarbons, phenols, chlorinated aliphatic compounds.

Conditions for the treatment of leachate water are prescribed by legal acts, and the application of treatment technology depends on the amount and composition of leachate water and the conditions of discharge into an open watercourse or public drainage system [4].

Mechanical, biological, and chemical purification procedures are used for wastewater treatment. Chemical purification processes are processes in which purification is carried out using certain chemical reactions or certain physical-chemical phenomena. The basic procedures of chemical wastewater treatment are the removal of certain dissolved substances: chemical precipitation, ion exchange, oxidation, aeration, and adsorption [5].

Adsorption is a diffusion operation by which one or more components are removed from the gas or liquid phase using solid porous materials, called adsorbents. A solid substance on the surface on which the adsorption process takes place is called an adsorbent, while the substance that binds is called an adsorbate [6].

Adsorption is performed under the influence of physical or chemical forces when the adsorbed ions or molecules come close enough to the adsorbent. Physical phenomena occur in the form of Van der Waals electrostatic forces. Chemical adsorption occurs when molecules on the surface of the adsorbent and adsorbate molecules react. The effect of adsorption depends on the total surface area of the grain by mass, i.e. of the specific surface area [7].

The most commonly used adsorbents in wastewater treatment are activated carbon, silica gel, zeolites, and more recently the so-called "low-cost" adsorbents (waste biomass such as sawdust of various types of wood, straws of various kinds of wheat, rice husks, walnut husks, hazelnut husks, stems and leaves of various types of plants, etc.) [8].

Clay minerals, including pyrophyllite, are highly valued for their adsorptive properties. The widespread use of clays in the industry for wastewater treatment applications is often recommended today due to their local availability, technical feasibility, engineering application, ions, and cost-effectiveness. [9].

Clay minerals appear as colloidal aggregates of small particles. Their large surface area is responsible for a number of unique physical and chemical properties such as cation exchange and pH-dependent sorption [10].

Pyrophyllite has shown great efficiency in the adsorption of heavy metals from contaminated wastewater as well as wastewater from electroplating plants. According to current regulations, the allowed pH value in wastewater from industrial plants before its discharge should be 7, which dictates the need for its neutralization before discharge into waterways. Optimizing the process of adsorption of heavy metals from the wastewater of the electroplating plant, it was concluded that the adsorption of metals is most favorable at a mass of pyrophyllite of 10 g, a fraction size of 0.10 mm, at pH 7, and a contact time of 2 hours [8, 11].

The results of the research into the effectiveness of raw and modified pyrophyllite (modified with boric acid) in the adsorption of heavy metals speak of the justification of further research, but also of the practical application of pyrophyllite in the purification of industrial wastewater. Analysis of waste and treated water also found that pyrophyllite treatment reduces: organic carbon, ammonia, total inorganic nitrogen, total phosphorus, and total alkalinity. The results showed the additional effectiveness of pyrophyllite on the reduction of organic compounds, indicating that pyrophyllite can be an effective agent for the treatment of wastewater in mines, the metal industry, and landfill leachate water [12].

Preliminary experimental results of heavy metal removal (Pb, Cu, Cd, Zn, and Ni) with PIR (pyrophyllite), PIR-B (pyrophyllite modified with boric acid,) and PIR-B-V (pyrophyllite modified with boric acid and washed with water) singled out pyrophyllite PIR as the most effective adsorbent, which has a particular affinity for lead: 47.25 mg/g, for the described operating conditions. This capacity stands out in relation to pyrophyllites from other sites. During the conduct of the experiment, the pH value was not adjusted, and during the sorption of lead ions, there was the smallest deviation between the initial and final pH values. Due to the fact that unmodified pyrophyllite was used without adjusting the pH value, the application itself is more economically profitable and simpler. Based on these experimental results, pyrophyllite can be used to remove lead from wastewater [13].

Chemical stabilization of soil contaminated with heavy metals using natural aluminosilicate materials (pyrophyllite and zeolite) has generally been shown to be a very effective measure from the point of view of reducing the accessibility of heavy metals in the soil, and therefore also from the point of view of reducing the possibility of their entering the plant, i.e. into the food chain. The results of this research support the thesis that zeolite, and especially pyrophyllite, have the ability to firmly bind heavy metals to their structure, which, on the one hand, reduces the possibility of their uptake by plants, and on the other hand, contributes to environmental protection, because by immobilizing heavy metals of metals reduces the possibility of their leaching from the surface layers of the soil into underground water courses [14, 15].

During the research, pyrophyllite proved to be a good adsorbent for glyphosate (organophosphorus herbicide), so in the future, it could be used as a filter in many experiments where it is necessary to examine the possibility and efficiency of adsorption [16].

Taking into account all previous research that was carried out on a laboratory-prepared sample contaminated with heavy metals, the goal of this work was to examine the effectiveness of pyrophyllite, as a heavy metal adsorbent, in the process of purifying waste landfill water.

2. MATERIALS AND METHODS

The removal of toxic metals from wastewater through the process of adsorption on natural materials such as clays is an efficient, inexpensive, and environmentally friendly procedure for preserving the environment. The material used in this work is pyrophyllite shale (hereafter pyrophyllite) from the Parsovići deposit, Konjic, Bosnia and Herzegovina. Pyrophyllite belongs to the group of aluminosilicate minerals of the chemical formula $Al_2Si_4O_{10}(OH)_2$, and in nature, it is found in the form of shale. It got its name from the Greek words *pir*-fire and *philon*-leaf because it spreads like a fan when heated. It is part of the isomorphic order of aluminosilicates that contain bound water. It is characterized by a three-layer crystal lattice, which has a tetrahedral structure in the outer layer, and an octahedral structure in the inner layer. The crystals are plate-like, soft, and greasy to the touch. It is electroneutral and not reactive in its natural form. Pyrophyllite is not soluble in water and does not swell. It is thermally stable. Depending on the admixture, the color of pyrophyllite varies from white, gray to purple. The chemical and mineralogical composition and physical properties of pyrophyllite are shown in Tables, 1, 2, and 3.

Table 1. Average chemical composition of pyrophyllite

Composition	SiO_2	Al_2O_3	Fe_2O_3	FeO	TiO_2	CaO	MgO	CO_2	Na_2O	K_2O	H_20^-	H_20^+	Other elements
%	61±	23.1±	1.1	0.25	0.12	1.85	1.94	4.30	0.61	1.44	0.61	4.66	<0.1

Table 2. Average physical properties of pyrophyllite

pH	8.0-9.0
Hardness (by Mohs)	1.0-1.5
Specific gravity g/cm^3	2.6-2.8
Volumetric weight without shaking (33 µm) u g/cm^3	0.380-0.420
Volumetric weight with shaking (33 µm) u g/cm^3	0.525-0.550
Volumetric weight without shaking (63 µm) u g/cm^3	0.508-0.530
Volumetric weight with shaking (63 µm) u g/cm^3	0.750-0.820

Table 3. Average mineralogical composition of pyrophyllite

Pyrophyllite	44-52 %
Quartz	12-18 %
Carbonates	10-12 %
Kaolinite	18-22 %
Serecit	6-12 %
Other minerals in smaller percentages	

Pyrophyllite has naturally hydrophobic properties on the surface in aqueous solutions, which acts as a neutral adsorption site, accessible for non-polar organic species. Edges are hydrophilic in aqueous solutions. Cation exchanges (e.g. Al^{3+} instead of Si^{4+} in the tetrahedral layer or Mg^{2+}, Fe^{2+}, Ti^{2+} instead of Al^{3+} in the octahedral layer) contribute to the negative charge which contributes to the adsorption of cations or organic polar pollutants.

Sampling of pyrophyllite was carried out at the site of the Parsovići mine, Konjic, Bosnia and Herzegovina. The pyrophyllite samples used were mechanically activated by crushing, grinding, and sieving. The effect of mechanochemical activation of pyrophyllite leads to significant changes in the mineral structure, i.e. to partial amorphization, due to an increase in the number of lattice defects and deformations in the crystal structure, which results in an increase in specific surface area and reactivity. During grinding, easy splitting of layers occurs, while ionic and covalent bonds in the structure are broken at the edges. This is why flat, layered surfaces are hydrophobic while edges are hydrophilic in aqueous solutions, forming negatively charged sites. Two granulation samples: 0-53 µm and 0-100 µm were used to test the adsorption of heavy metals in this work.

Leachate landfill water was sampled at the sanitary municipal landfill "Desetine", Tuzla. The basic characteristics of landfill soil are the structure of sediments: clay, marl, sandstone, conglomerate, and sand. Clays and marls, i.e. the zones they build act as a hydrogeological insulator, while the zone with conglomerates, sand, and sandstones represent a collector of integral porosity. The greater the thickness of the clay and the greater its density, the greater the effect of purifying the filtrate. All leachate water from the waste material and from the surface, porous soil located on the impermeable layer is collected by a drainage system and controlled under an earthen dam [17]. Collected wastewater does not undergo any purification treatment before discharge into the recipient, surface water.

Parameters that exceed the permitted limit value in relation to the current legal regulation are heavy metals: Fe, Ni, Mn, and biological oxygen demand (BOD_5). In this paper, the focus of purification is on the removal of heavy metals to the satisfactory values prescribed by Regulation [4].

Heavy metal adsorption experiments were performed using the "Batch" method, direct contact of a certain amount of pyrophyllite, and a real sample of landfill leachate in the Laboratory of AD Harbi LLC, Sarajevo.

3. EXPERIMENTAL PART

Visual characteristics of the initial sample of landfill leachate water: dark yellow, slightly turbidity water with a very sharp and unpleasant smell.

The leachate water is divided into three parts for further treatment:

- **Sample 1** - landfill water without treatment,
- **Sample 2** - landfill water for treatment with pyrophyllite granulation 0-53 µm in a concentration of 5%,
- **Sample 3** - landfill water for treatment with pyrophyllite granulation 0-100 µm in a concentration of 5%.

The laboratory equipment used was a laboratory balance, a magnetic stirrer type Velp Scientifica, an electric vacuum pump type KNF Neuberger and other standard laboratory accessories and dishes. Pyrophyllite granulation 0-53 µm and 0-100 µm in a concentration of 5% were added to water samples 2 and 3, after which they were mixed on a laboratory stirrer at a speed of 200 rpm, for 2 hours (Figures 1a, b, and c).

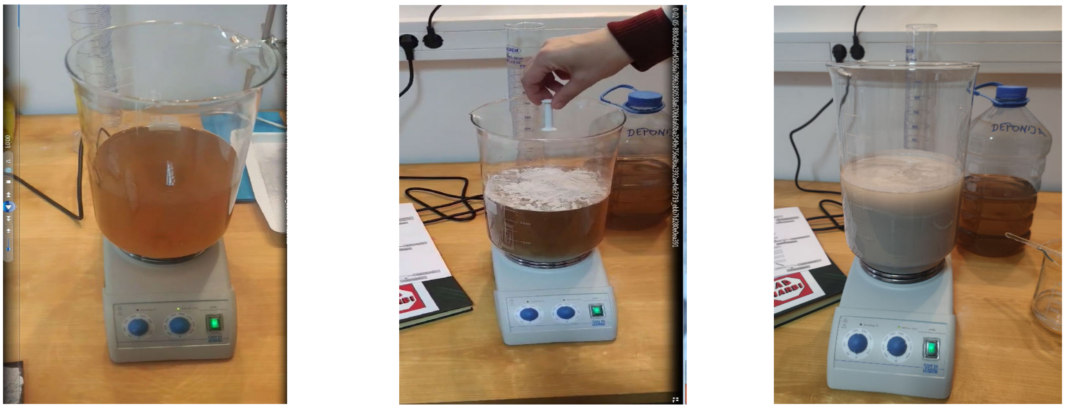
a) b) c)

Figure 1. Sample of landfill leachate water before (a), during (b), and after (c) the addition of pyrophyllite

At the end of 2 hours, the mixture of wastewater and pyrophyllite was filtered on a Büchner funnel, through a filter paper blue strip with the use of an electric vacuum pump, for assisted filtration. The treatment was repeated twice with both granulations of pyrophyllite, by adding the same amount of pyrophyllite (concentration 5%) to the filtrates after the first treatment.
Laboratory determination of the content of iron, nickel, and manganese in leachate landfill water was done in cooperation with the Laboratory of the Institute of Chemical Engineering Tuzla, using standard methods EPA Method 7000 B and BAS ISO 11047:2000. Both mentioned methods are based on flame atomic absorption spectrophotometry, and instruments manufactured by Perkin Elmer, type Optima 2100 DV (optical emission spectrometer-plasma) and manufactured by VARIAN, type AA 200 (Atomic Absorption Spectrometer) were used for testing.

4. RESULTS AND DISCUSSION

Below is a tables and charts overview of experimentally obtained results.

Table 4. Initial and limiting pH values and metal values

Metal	Concentration in the initial water sample (mg/l)	* Limit value for surface water bodies (mg/l)
Fe	2.766	2.0
Ni	0.656	0.5
Mn	3.307	1.0
pH	7.12	6.5-9.0

** in accordance with the applicable legislation, Annex 1. [4]*

Table 5. pH value, metal concentrations in the initial sample of landfill leachate water, and after Ist and IInd treatment with pyrophyllite granulation 0-53 µm

Metal	Concentration in initial sample (mg/l)	I treatment (mg/l)	II treatment (mg/l)
Fe	2.766	<0.006	<0.006
Ni	0.656	0.117	0.108
Mn	3.307	1.096	0.201
pH	7.12	7.42	7.63

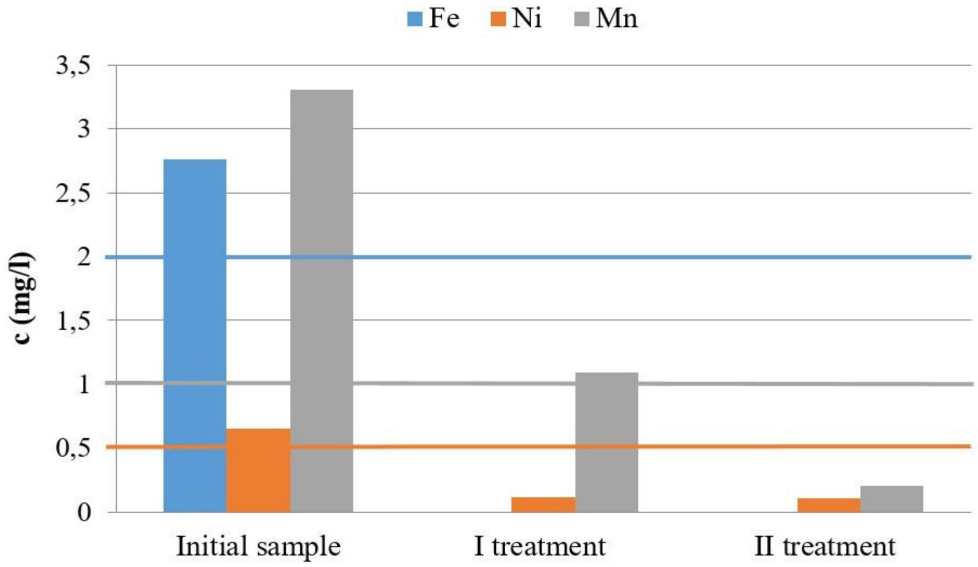

Figure 2. Presentation of limiting metal concentrations, metal concentrations in the initial sample of leachate landfill water and after Ist and IInd treatment with pyrophyllite granulation 0-53 μm

Table 6. pH value, metal concentrations in the initial sample of leachate landfill water after Ist and IInd treatment with pyrophyllite granulation 0-100 μm

Metal	Concentration in initial sample (mg/l)	I treatment (mg/l)	II treatment (mg/l)
Fe	2.766	0.231	<0.006
Ni	0.656	0.200	0.107
Mn	3.307	0.665	0.198
pH	7.12	7.37	7.44

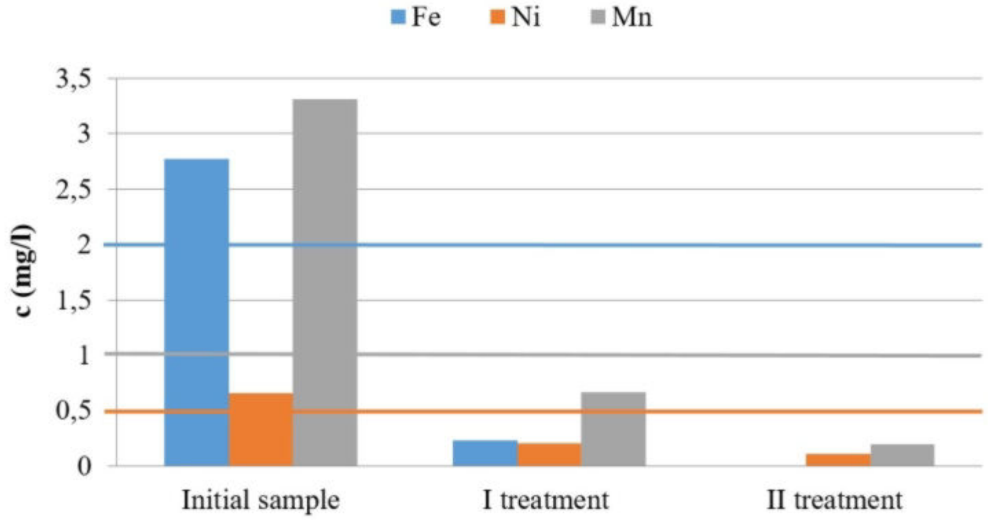

Figure 3. Presentation of limit concentrations of metals, the concentration of metals in the initial sample of landfill leachate water after Ist and IInd treatment with pyrophyllite granulation 0-100μm

Table 7. Overview of adsorption efficiency depending on pyrophyllite granulation

Metal	% adsorption			
	Ist treatment 0-53 µm	Ist treatment 0-100 µm	IInd treatment 0-53 µm	IInd treatment 0-100 µm
Fe	100.0	91.6	0	100
Ni	82.2	69.5	7.7	46.5
Mn	66.9	79.9	81.7	70.2

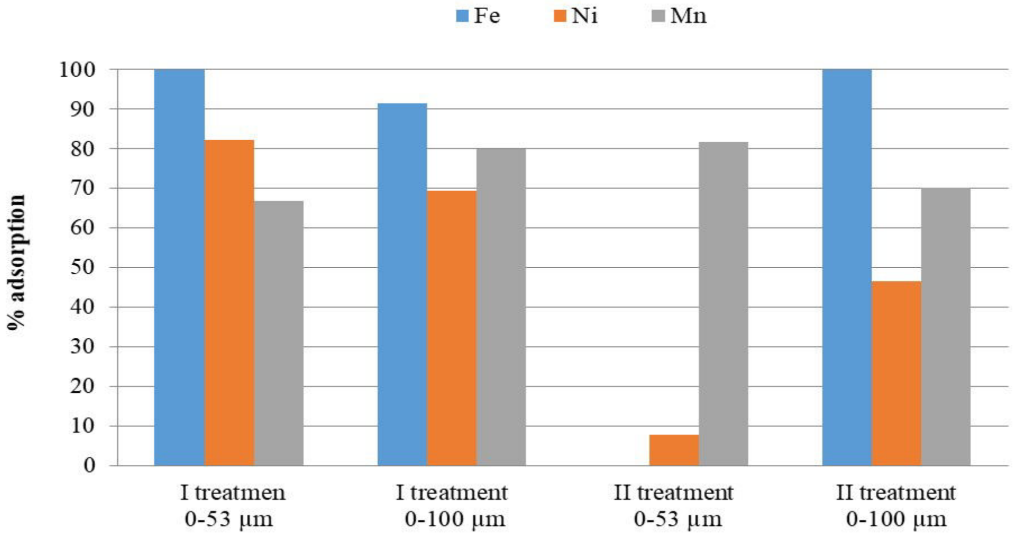

Figure 4. Presentation of adsorption efficiency depending on granulation

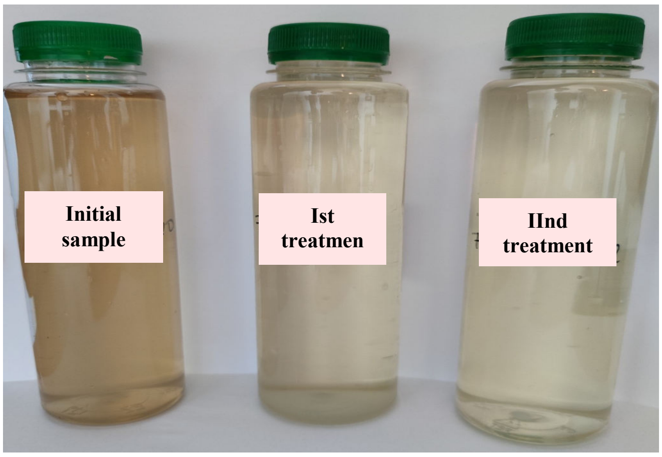

Figure 5. Visual representation of samples of landfill leachate before and after treatments

After the first treatment, the unpleasant smell was significantly reduced in both treated samples, and after the second it was almost gone. As leachate water is rich in ammonia compounds, with an intense smell, it is clear that pyrophyllite plays a role in binding them and neutralizing the smell. After both treatments of landfill leachate with pyrophyllite, a lighter color of the sample is observed, as seen in Figure 5.

When it comes to the change in pH value, the initial sample had a value of 7.12, and after the IInd treatment, the pH value was 7.63 (for granulation 0-53 µm) and 7.44 (for granulation 0-100 µm). An increase in pH, i.e. alkalinity of the environment, indicates an increase in hydroxyl ions and cations as a consequence of adsorption chemistry.

The results of the experiment conducted on Sample 1 (pyrophyllite granulation 0-53 µm) are shown in Table 5 indicate a decrease in the concentration of iron from the initial value of 2.766 mg/l to a value less than 0.006 mg/l immediately after the I treatment, the concentration of nickel from the initial value 0.656 mg/l to a value of 0.117 mg/l after the Ist treatment or 0.108 mg/l after the IInd treatment, and manganese concentration from the initial value of 3.307 mg/l to a value of 1.096 mg/l after the Ist treatment or 0.201 mg/l after the IInd treatment.

The results of the experiment conducted on Sample 2 (pyrophyllite granulation 0-100 µm) shown in Table 6 indicate a decrease in iron concentration from the initial value of 2.766 mg/l to a value of less than 0.231 mg/l after the first treatment, i.e. to a value of less than 0.006 mg/l after the IInd treatment, nickel concentrations from the initial value of 0.656 mg/l to a value of 0.200 mg/l after the Ist treatment, i.e. 0.107 mg/l after the IInd treatment, and manganese concentrations from the initial value of 3.307 mg/l to a value of 0.665 mg/l after the first treatment or 0.198 mg/l after the second treatment.

5. CONCLUSION

The results of the research prove that pyrophyllite from the "Parsovići" deposit, Konjic, Bosnia and Herzegovina, can be used as an effective agent (adsorbent) for removing iron, nickel, and manganese from the landfill leachate taken from the sanitary landfill "Desetine" in Tuzla (Figures 2, 3, and 4).

The paper examined the effectiveness of two granulations of pyrophyllite (0-53 µm and 0-100 µm) on the degree of adsorption of heavy metals, Fe, Ni, and Mn present in landfill leachate water.

The research results indicate that the iron in the sample can be completely removed immediately after the first treatment with pyrophyllite of both pyrophyllite granulations (granulation 0-53 µm) and (granulation 0-100 µm).

The removal of nickel from landfill leachate water was achieved immediately after the first treatment with pyrophyllite in the amount of 82.2% (for granulation 0-53 µm) and 69.5% (for granulation 0-100 µm) in relation to the initial concentration. The stated efficiency in both cases indicates that the remaining concentrations of nickel in leachate landfill water are below the permitted limit value and that this leachate can be discharged into the final recipient without further treatment. The IInd treatment with pyrophyllite for the purpose of reducing nickel in this water was not even necessary.

Manganese in the landfill leachate sample exceeded the permitted limit value the most (up to 3 times) and its removal from the landfill leachate water required both treatments. Better adsorption efficiency in the amount of 79.9% was shown by the coarser granulation of the used pyrophyllite (0-100 µm) after the first treatment, while in the second treatment, the efficiency was better with the granulation 0-53 µm and was 81.7% compared to initial sample.

When using both granulations, manganese was removed from the landfill leachate water, and the remaining concentrations were below the legally prescribed values.

Bearing in mind the number of sanitary landfills in Bosnia and Herzegovina and the region, which represent an increasing environmental problem and challenge, and the fact that they do not have any leachate treatment, pyrophyllite as a valuable natural mineral with proven adsorption properties is emerging as an effective ecological and innovative solution to the problem of pollution heavy metals.

Acknowledgement

We hereby express our gratitude to our professional associates and scientific advisors for their unselfish professional support and research that contributed to proving the adsorption capacity of pyrophyllite shale: Dr. Mirjana Stojanović, Dr. Milan Adamović, Ph.D. Jasmina Grbović-Novaković, Ph.D. Tanja Trtić-Petrović, Dr. Ljubiša Andrić, Ph.D. Dragan Radulović, Ph.D. Nedžad Alić, Ph.D. Suzana

Atlagić-Gotovac, Ph.D. Dijana Jelić, Ph.D. Ahmed Džubur, Ph.D. Senad Murtić, Ph.D. Emina Sijahović, Ph.D. Lejla Klepo, Ph.D. Jasna Huremović, and Dr. Tidža Muhić-Šarac.

Conflict of interest

The authors declare that they have no competing interests.

6. References

[1] A. Serdarević, Izbor procesa prečišćavanja procjednih voda sanitarnih deponija, *Vodoprivreda*, 49(2017) 288-290, p. 297-304

[2] A. Serdarević, Upravljanje procjednim vodama: produkcija, sastav, prikupljanje i obrada, Upravljanje procjednim vodama: produkcija, sastav, prikupljanje i obrada, Svjetski dan voda, Agencija za vodno područje rijeke Save, Zenica, 22.-23.3.2017., (izlaganje)

[3] A. Buzdovačić, *Obrada procjedne vode odlagališta otpada primjenom šaržnog hibridnog procesa korištenjem prirodnog zeolita*, [Završni rad], Sveučilište u Splitu, Kemijsko-tehnološki fakultet, Odsjek za hemiju, 2018.

[4] *Uredba o uslovima ispuštanja otpadnih voda u okoliš i sisteme javne kanalizacije*, Službene novine Federacije BiH, br. 26/20 i *Uredba o izmjenama i dopunama Uredbe o uslovima ispuštanja otpadnih voda u okoliš i sisteme javne kanalizacije,* Službene novine Federacije BiH, br. 96/20

[5] R. Kitanović, V. Šušteršič, Tretman otpadnih voda, *Vojnotehnički glasnik/Military technical courier*, 61(2013) 3, p.122-140

[6] I. Šetka, *Obrada otpadnih voda nakon postupka galvanizacije metala*, [Magistarski rad], Univerzitet u Zagrebu, Rudarsko-geološko-naftni fakultet, Odsjek za hemiju, Zagreb, 2014.

[7] Š. Goletić, N. Imamović, N. Avdić, *Obrada otpadnih voda*, Univerzitet u Zenici, 2014.,

[8] E. Kulović, Utvrđivanje kapaciteta adsorpcije teških metala iz otpadne vode na pirofilitu, [Magistarski rad], Univerzitet u Sarajevu, Prirodno-matematički fakultet, Odsjek za hemiju, Sarajevo, 2017.

[9] M. Erdemoğlu, S. Erdemoğlu, F. Sayılkan, M. Akarsu, Ş. Şener & Sayılkan, Organo-functional modified pyrophyllite: preparation, characterisation and Pb(II) ion adsorption property, *Applied Clay Science*, *27*(2004) 1-2, p. 41-52

[10] S. V. Churakov, Ab initio study of sorption on pyrophyllite: Structure and acidity of the edge sites, *The Journal of Physical Chemistry B*, 110(2006) 9, p. 4135-4146

[11] N. Halilović, *Optimizacija procesa adsorpcije teških metala iz otpadne vode na pirofilitu*, [Magistarski rad], Univerzitet u Sarajevo, Prirodno-matematički fakultet, Odsjek za hemiju, Sarajevo, 2018.

[12] T. Trtić-Petrović, I. Pušica, M. Purenović, Đ. Vaštoh, *Mechanically and chemically modified pyrophyllite for removal of heavy metals from aqueous solutions*, Book of Abstracts, VIIth International Congress Engineering, Environment and Materials in Process Industry, Jahorina, March 17-19, 2021, [ed. M. Gligorić, D. Vujadinović and M. Beribaka], Onlajn izd. - El. zbornik, Zvornik

[13] Z. Lopičić, J. Milojković, D. Radulović, *Studija ispitivanja rovnog i modifikovanog pirofilita „Parsovići" i njihove moguće primene u uklanjanju teških metala*, Institut za nuklearne i druge mineralne sirovine, 2019., Beograd

[14] H. Čivić, S. Murtić, E. Sijahović, *Elaborat o modelima zaštite i remedijacije zemljišta onečišćenim teškim metalima u industrijskim područjima Federacije Bosne i Hercegovine*, Univerzitet u Sarajevu, Poljoprivredno-prehrambeni fakultet, 2020., Sarajevo

[15] S. Murtić, H. Čivić, E. Sijahović, I. Koleška, J. Jurković, M. Tvica, Use of pyrophyllite to reduce heavy metals mobility in a soil environment, *Agron. Res.*, (2020) 18, p. 194–205

[16] N. Boloban, *Spektrofotometrijsko određivanje glifosata i njegova adsorpcija na pirofilitu*, [Završni rad], Univerzitet u Sarajevo, Prirodno-matematički fakultet, Odsjek za hemiju, Sarajevo, 2020.

[17] Služba za komunalne poslove, izgradnju i poslove mjesnih zajednica, Centar za ekologiju i energiju, *Plan upravljanja otpadom za grad Tuzla, 2017–2022*, Juni, 2017.

JST&M 4(2023), 16 - 21
DOI: 10.57131/jstm.2023.4.3

JST&M

cc BY

Original scientific paper

ANALYSIS OF PRODUCTION METHOD AND STABILIZING AGENT ON STRUCTURE OF ALUMINUM METAL FOAMS

Karla Grgić, Igor Ćulum, Branimir Lela, Jure Krolo, Sonja Jozić

University of Split, Faculty of Electrical Engineering, Mechanical Engineering, and Naval Architecture

ABSTRACT

Aluminium alloy foams are a form of porous metal whose structure resembles the shape of natural materials such as coral, bone, sponge, etc. Due to their structure, these materials retain good mechanical properties of the base material while being significantly lighter than non-porous metal. Metal foams can be used as energy and vibration absorbers, heat exchangers, insulators, and filters. The main disadvantage of this type of material is its high production cost. To reduce production costs, aluminium alloy chips are used as base material. Foams are made of A360 and AA 7075 aluminium alloys. To produce a porous structure, $CaCO_3$ is used as a foaming agent while Zn and CaO were added as stabilizing agents. The main goal of the paper was to investigate the difference in the shape of pores and relative density after foaming with different stabilizing agents.

Keywords: metal foam, chip waste, recycling, relative density, stabilizer

Corresponding Author:
Karla Grgić
Faculty of Electrical Engineering, Mechanical Engineering, and
Naval Architecture, University of Split Ruđera Boškovića 32, 21 000 Split
Republic of Croatia
Tel: +385 21 305931
E-mail address: Karla.Grgic.00@fesb.hr

1. INTRODUCTION

Metal foams imitate the structure of coral, sponge, and bone [1] and can be made from materials such as aluminium, titanium, nickel, and polymers [2]. They are characterized as low-density materials with high energy and sound absorption. Foams are divided into two groups, with open and closed cells. Open cell foams are made by compacting base material and space holder. After that material is heated and the space holder leaks [3]. These types of foams are used as filters, heat exchangers, and electrodes [4]. Closed-cell foams are made by compacting alloy powder and foaming agents such as TiH_2, $CaCO_3$, and others [5]. They can be made with hot compaction or extrusion. After that process, samples are heated depending on the foaming agent. Titanium hydride's decomposition temperature is close to the melting point of aluminium alloy thus making it an optimal foaming agent. Calcium carbonate, however, is much cheaper and, due to higher decomposition temperature, requires no pre-treatment which leads to lower production costs [6,7,8].

Movahedi et. al proved that foaming with calcium carbonate gives smaller pores, even though temperature, foaming time, and $CaCO_3$ concentration were higher. Foams produced with $CaCO_3$ have greater compression strength and energy absorption, but lower density [9]. Sudharsan et. al proved that adding Mg and Cu, increased the wettability and stability of the foams. It is important to avoid premature gas release [10]. Wang et al. used the pre-oxidation process by heating TiH_2 to postpone gas release at lower temperatures [11]. Carbon dioxide gas stabilizes the foam and prevents coagulation. The difference between TiH_2 and $CaCO_3$ foaming agents is that $CaCO_3$ has a greater decomposition temperature which is needed for the foaming process [12,13].

The most common starting material for aluminium foam production is aluminium powder. The costs associated with this base material lead to a drastic increase in the overall production cost [14]. Using chips that are a by-product of the different machining processes could significantly decrease the production cost of these types of materials. The main challenge in producing foams from aluminium chips is the mixing of larger alloy chip waste and small powder grains of foaming agents. Tsuda et al. analyzed the influence of different base materials on pore sizes. Their research concluded that foams produced with powder alloy have a more homogeneous structure than foams produced using alloy chip waste [15].

The goal of this paper is to analyze the expansion and shape of aluminium foam pores produced using different weight percentages of $CaCO_3$ foaming agent. This paper is an extension of the previous article in which differences between foaming with TiH_2 and $CaCO_3$ were given [16].

2. EXPERIMENTAL WORK

Materials used for foam production were aluminium alloy chips A360 and AA 7075. Chips were produced on vertical machining center Spinner VC 560. The cutting tool and cutting parameters used for chip production of both alloys were the same to keep the chip dimensions comparable. The samples were split into groups: first to be compacted and second to be extruded. A certain percentage of foaming agent ($CaCO_3$) and stabilizing agents (CaO or Zn) was mixed with the aluminium alloy chips. The correct weight percentages of the foaming and stabilizing agents are shown in Table 1. Firstly, the mixture of both groups was cold compacted with a force of 400 kN. Compression force was measured with the HBM load cell C6A 1MN sensor.

Table 1. Production parameters

Sample number	Process	Alloy	Foaming and stabilizing agent	Foaming temperature (°C)	Foaming time (min)
1	Extrusion	A360	5% $CaCO_3$ + 2% Zn	800	15
2	Extrusion	AA 7075	5% $CaCO_3$ + 2% Zn	800	15
3	Extrusion	A360	5% $CaCO_3$ + 2% CaO	800	15
4	Extrusion	AA 7075	5% $CaCO_3$ + 2% CaO	820	15
5	Extrusion	A360	5% $CaCO_3$ + 2% Zn	820	15
6	Extrusion	AA 7075	5% $CaCO_3$ + 2% Zn	820	15
7	Compaction	A360	3% $CaCO_3$ + 2% Zn	800	20
8	Compaction	AA 7075	3% $CaCO_3$ + 2% Zn	800	20

After cold compacting, the samples from the first group were hot compacted. The process started with heating in the furnace for 20 minutes at a temperature of 420 °C. The furnace used to heat the sample was Demiterm Easy 9. After the heating process, the sample was put in the hydraulic press. The mould used for the compression was heated to 400 °C. After that, the sample was hot pressed with a force of 400 kN. Omron temperature regulator E5CC and a relay G3PE-225B DC12-24 were used for measuring the temperature. Finally, the samples were placed in a mould with a diameter of 40 mm and heated to foaming temperatures.

The second group of samples was hot extruded with previous heating in the furnace at the same temperature as the first group. They were also foamed at similar temperatures which are visible in Table 1. The mould used for the foaming of the second group was 22 mm in diameter.

Relative density can be calculated as a ratio of foams density (ρ_f) and the density of aluminium alloy (ρ_s) [17].

$$\rho = \frac{\rho_f}{\rho_s} \tag{1}$$

3. RESULTS

Table 2 shows the results of the calculated relative density. It can be seen that the density of compacted samples is higher in comparison with extruded samples. The main reason is the higher percentage of $CaCO_3$ in the extruded samples. In comparison with the previous research [16], relative densities are as low as 0,26. The important difference between these two analyses is the addition of Zn as a stabilizing agent.

It can be concluded that Zn promotes higher expansion, even though the amount of foaming agent is very low at just 3%. There is a small difference in relative density comparing two alloys A360 and AA 7075 with the same temperature and time of foaming. Because of the higher decomposition temperature of $CaCO_3$, different liquidus temperatures of aluminium alloys are not an influencing factor in the process.

From Table 2 it can be concluded that foams with the addition of CaO have the highest density of extruded samples. Because of that, this stabilizing agent was not used in the process of compaction. High relative densities with CaO can be attributed to the high oxide level in the material during foaming that prevents foam expansion. Oxides help to stabilize the foams, but in this process, they are already present after the decomposition of calcium carbonate into CO_2.

Table 2. Relative density

Sample number	Process	Alloy	Foaming and stabilizing agent	Foaming temperature (°C)	Foaming time (min)	Relative density
1	Extrusion	A360	5% $CaCO_3$ + 2% Zn	800	15	0,26
2	Extrusion	AA 7075	5% $CaCO_3$ + 2% Zn	800	15	0,286
3	Extrusion	A360	5% $CaCO_3$ + 2% CaO	800	15	0,41
4	Extrusion	AA 7075	5% $CaCO_3$ + 2% CaO	820	15	0,39
5	Extrusion	A360	5% $CaCO_3$ + 2% Zn	820	15	0,337
6	Extrusion	AA 7075	5% $CaCO_3$ + 2% Zn	820	15	0,289
7	Compaction	A360	3% $CaCO_3$ + 2% Zn	800	20	0,442
8	Compaction	AA 7075	3% $CaCO_3$ + 2% Zn	800	20	0,53

Comparing samples 1 and 5 which are made of A360, it can be concluded that higher density is achieved when using a higher temperature of 820 °C. The reason for this can be the coagulation of foams at higher temperatures and the same foaming times, Figure 1.

Similar results are found in samples 2 and 6 even though this difference is far lower. At lower temperatures, sample 2 with AA 7075 has a higher relative density than sample 1. When comparing samples foamed at a higher temperature, the opposite was observed. This can be due to the end of the expansion of A360 at a lower temperature. After that, foam coagulates and leaks, and the density rises.

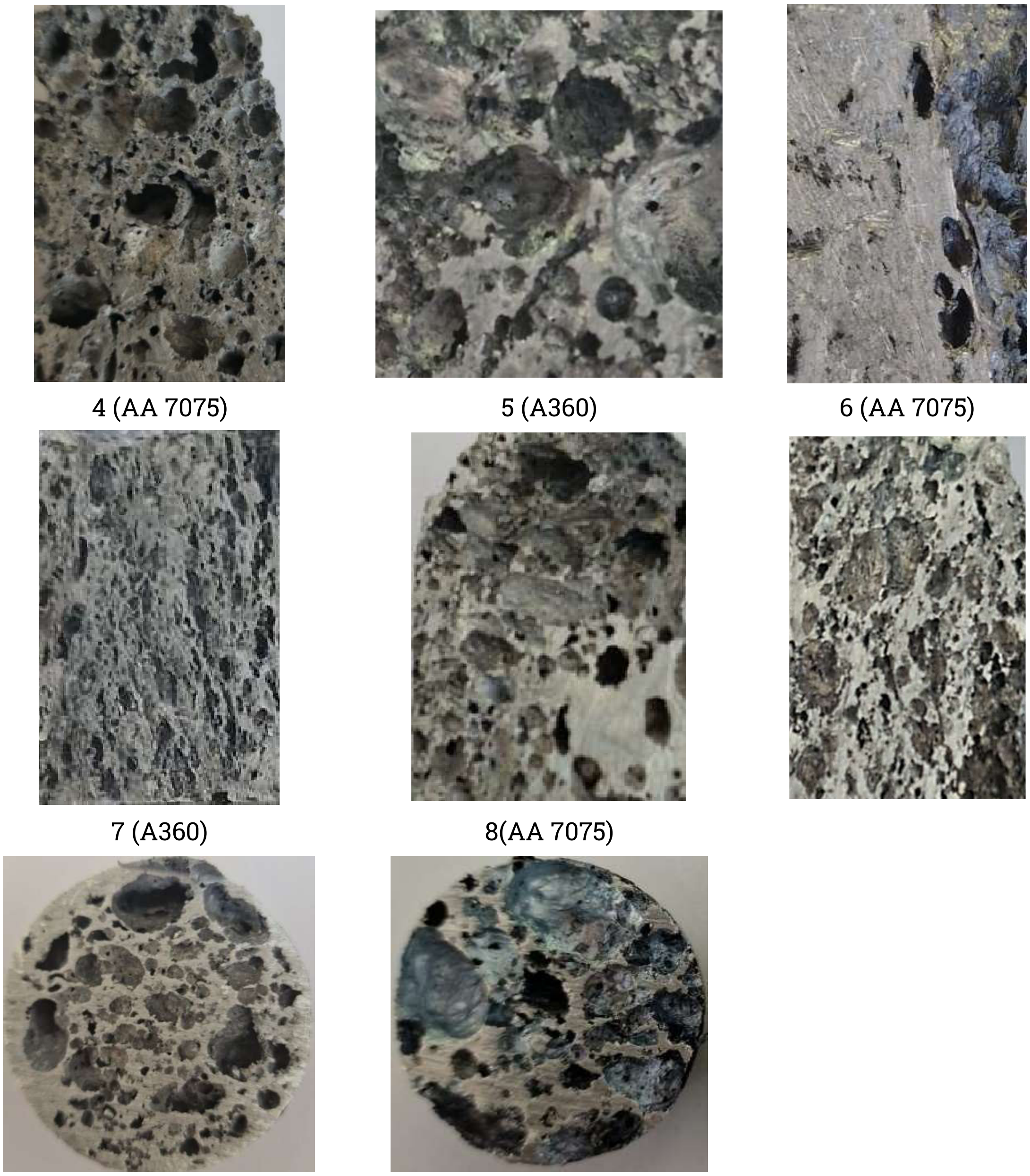
1 (A360) 2 (AA 7075) 3 (A360)

4 (AA 7075) 5 (A360) 6 (AA 7075)

7 (A360) 8(AA 7075)

Figure 1. Structure of samples

Sample 4, made with CaO, has a structure that is horizontal with the foaming direction. This foam has no rounded and homogenous pores 1. It is also similar to sample 3 which has only a few larger pores directed in the same way as sample 4. Because of this inhomogeneous structure of foams, CaO was not used as a stabilizer for the compacted samples. As it was mentioned previously, calcium carbonate decomposes to CO_2 and the addition of CaO raises the viscosity of samples. Generally, oxides to one limit act as stabilizing agents, however, the viscosity in this sample is too high and prevents grow of foams.

Samples with zinc as a stabilizing agent have more rounded pores and structure that is not directed in one way. The first sample has the most homogenous structure out of the extruded samples. It can be concluded that A360 is more convenient for foaming with this stabilizing and foaming agent than AA 7075. That is confirmed by Figure 1, where samples 1, 5, and 7 have a more rounded structure. Samples 7 and 8 have rounded pores that are not directed.

A more uniform structure was obtained due to a lower concentration of $CaCO_3$. Several larger pores can be related to powder accumulation at the beginning of the process.

4. CONCLUSION

In this paper production of aluminium foams using various production processes and stabilizing agents were analyzed. Aluminium A360 and AA 7075 chip waste were used in the foaming process together with $CaCO_3$ as a foaming agent. Additionally, Zn and CaO were used as stabilizing agents. Analyzing the pores and relative densities of the produced foams, the following was concluded:

- Samples with CaO had an inhomogeneous structure that is related to higher oxide levels in the foam. Oxides act as stabilizers, but with a higher percentage, they raise the viscosity and prevent expansion.
- Zinc helps to stabilize the foams, and using this agent pores are more rounded than in samples 3 and 4 with CaO.
- Foams 7 and 8 had the highest density because of the lower $CaCO_3$ percentage. Rounded pores were also observed.
- The higher temperature of foaming leads to higher relative density. That can relate to an increase in pore diameter which can cause coagulation and leakage.
- At lower temperatures, sample 1 with A360 has a lower density than sample 2 with AA 7075, and at higher temperatures, there is a higher density with A360 foam.

Acknowledgement

This research has been supported by The Croatian Science Foundation through the project ALURECSS (IP-2020-02-8284).

Conflicts of Interest

The authors declare no conflict of interest

5. References

[1] M. F. Ashby, A. Evans, N. A. Fleck, L. J. Gibson, J. W. Hutchinson, H. N. Wadley, Metal foams: a design guide, Vol. 23, No. 1. 2002

[2] E. Prados Martín, Microstructural parameters affecting the compressive response of closed-cell aluminum foams, *Mech. Adv. Mater. Struct.*, 0(2021) 0, p. 1–20, doi: 10.1080/15376494.2021.1872747

[3] H. Ali, A. Gábora, M. A. Naeem, G. Kalácska, T. Mankovits, Effect of the manufacturing parameters on the pore size and porosity of closed-cell hybrid aluminum foams, *Int. Rev. Appl. Sci. Eng.*, 12(2021) 3, p. 230, doi: 10.1556/1848.2021.00262

[4] A. Bisht, B. Gangil, Structural and physico-mechanical characterization of closed-cell aluminum foams with different zinc additions, *Sci. Eng. Compos. Mater.*, 25(20178) 4, p. 789–795, doi: 10.1515/secm-2016-0307

[5] R. Karuppasamy, D. Barikm, Production methods of aluminium foam: A brief review, *Mater. Today Proc.*, 37,/(2020) Part 2, p. 1584–1587, 2020, doi: 10.1016/j.matpr.2020.07.161

[6] D. P. Papadopoulos, H. Omar, F. Stergioudi, S. A. Tsipas, N. Michailidism, The use of dolomite as foaming agent and its effect on the microstructure of aluminium metal foams-Comparison to titanium hydride, Colloids Surfaces, *A Physicochem. Eng. Asp.*, 382(2011) 1–3, p. 118–123, doi: 10.1016/j.colsurfa.2010.12.005

[7] J. An, C. Chen, M;. Zhang,m Effect of CaCO3 content change on the production of closed-cell aluminum foam by selective laser melting, *Opt. Laser Technol.*, 141(2021), p. 107097, doi: 10.1016/j.optlastec.2021.107097

[8] V. Kevorkijan, S. D. Skapin, I. Paulin, B. Sustarsic, M. Jenkom, Synthesis and Characterisation of Closed Cells Aluminium Foams Containing Dolomite Powder As

Foaming Agent, *Mater. Tehnol.*, 44/(2010) 6, p. 363–371

[9] N. Movahedi, S. M. H. Mirbagherim, Comparison of the Energy Absorption of Closed-Cell Aluminum Foam Produced by Various Foaming Agents, *Strength Mater.*, 48(2016) 3, p. 444–449, doi: 10.1007/s11223-016-9783-y

[10] N. Sudharsan, T. Rajasekaran, and G. S. Vinod-Kumar, Optimizing the hot compaction parameters of Al-Mg-Cu foams processed through elemental powder route, *IOP Conf. Ser. Mater. Sci. Eng.*, 402(2018) 1, doi: 10.1088/1757-899X/402/1/012202

[11] H. Wang, D. F. Zhu, S. Hou, D. H. Yang, T. G. Nieh, Z. P. Lu, Cellular structure and energy absorption of Al–Cu alloy foams fabricated via a two-step foaming method, *Mater. Des.*, 196(2020), doi: 10.1016/j.matdes.2020.109090

[12] A. H. Jaafar, H. Al-Ethari, K. Farhan, Modelling and optimization of manufacturing calcium carbonate-based aluminum foam, *Mater. Res. Express*, 6(2019) 8, doi: 10.1088/2053-1591/ab2602.

[13] T. N. Praveen Kumar, S. Venkateswaran, S. Seetharamu: Effect of Grain Size of Calcium Carbonate Foaming Agent on Physical Properties of Eutectic Al–Si Alloy Closed Cell Foam, *Trans. Indian Inst. Met.*, 68(2015) 1, p. 109–112, doi: 10.1007/s12666-015-0631-8

[14] G. S. V. Kumar, F. García-Moreno, J.Banhart, A. Kennedym, The stabilising effect of oxides in foamed aluminium alloy scrap*, Int. J. Mater. Res.*, 106(2015) 9, p. 978–987, doi: 10.3139/146.111255

[15] S. Tsuda, M. Kobashi, N. Kanetake, Producing technology of aluminum foam from machined chip waste, *Mater. Trans.*,. 47(2006) 9, p. 2125–2130, doi: 10.2320/matertrans.47.2125

[16] K. Grgić, B. Lela, S. Jozić, J. Krolom, Aluminium foams made of various aluminium alloys scrap and various foaming agents, 2022, Proc. of 11th Int. Conf. Mechanical Technology and Structural Materials, ed. S. Jozić, B. Lela and N. Gjeldum, [Croatia: Croatian society for mechanical technologies]

[17] M. R. Farahani, H. R. Rezaei Ashtiani, S. H. Elahim, Effect of Zinc Content on the Mechanical Properties of Closed-Cell Aluminum Foams*, Int. J. Met.*, 16(2021) 6, p. 713-722, doi: 10.1007/s40962-021-00635-2.

JST&M 4(2023), 22 - 29
DOI: 10.57131/jstm.2023.4.4

Original scientific paper

EFFECT OF PARTICLE SHAPE AND SIZE OF COPPER POWDERS ON THE PROPERTIES OF SINTERED PARTS

Ivana Marković[1], Stevan Trujić[2], Dragan Manasijević[1], Ljubiša Balanović[1], Uroš Stamenković[1], Milijana Mitrović[1],

[1]University of Belgrade, Technical Faculty in Bor
[2]HBIS Group Serbia Iron & Steel

ABSTRACT

The particle shape and size of the starting powders represent the most important physical properties, on which the quality of the compacts and final sintered products depends. Two types of powder were analyzed in the paper - electrolytic copper powder with a dendritic particle shape and water-atomized copper powder with an irregular particle shape. The starting powders were sieved through a sieve system with openings of 45 µm, 80 µm, and 120 µm. The characterization of the obtained fractions of both powders was performed by determining the shape and dimensions of the particles using SEM microscopy in combination with ImageJ software, and the apparent density and flow rate were determined using the Hall flowmeter funnel. Pressing of each powder fraction was done using a pressure of 600 MPa. The compacts were further sintered at 1000°C for 2 hours to obtain the final sintered parts. After sintering, their density, hardness, and electrical conductivity were determined and their microstructure was analyzed. The results indicate a great influence of the characteristics of the starting powders on the properties of the final parts obtained by the powder metallurgy route. The particle shape of the powders had a more pronounced influence compared to the particle size.

Keywords: electrolytic powders, water-atomized powders, sintering, particle size, shape

Corresponding Author:
Ivana Marković
University of Belgrade, Technical Faculty in Bor
Vojske Jugoslavije 12, Bor, Serbia
Tel: +381 30 424 555
E-mail address: imarkovic@tfbor.bg.ac.rs

1. INTRODUCTION

The powder metallurgy (PM) route includes obtaining the final products through compact the starting powders and sintering them under controlled conditions. The main disadvantage of the classical PM process is the impossibility of achieving a full density of final products, due to their porosity, and that is why the mechanical properties of sintered parts are lower [1, 2]. Properties of sintered parts depend on the parameters such as characteristics of the starting powders, compaction pressure, sintering temperature and time, etc. If the compaction pressure, sintering temperature, and time are higher, the density is superior, and the porosity is lower. Mechanical and electrical properties are also dependent on the density and porosity, therefore, they increase with an increase in compaction pressure, sintering temperature, and time, but all this increases the process cost [3].

In addition to the process parameters, the particle shape and size have a great influence on all operations during obtaining parts using the PM route and on the quality of the final sintered products. The particle shape has a large effect on the contacts between particles and therefore has a significant influence on their behavior during pressing and sintering. Generally, the compacts obtained from coarse powder particles have a higher density compared with the compacts from fine powders [4].

To obtain the required properties in the final sintered parts, a suitable combination of process parameters is required [5, 6]. This paper presents the effects of particle shape and size of the starting copper powders, on the properties of powders, green compacts, and sintered samples. In the case of powders, the evaluated properties were apparent density and flow rate. In green compacts, density was evaluated, and in sintered samples hardness, electrical conductivity, and microstructure of PM parts were discussed. To obtain samples with different average particle sizes, water-atomized and electrolytic copper powders were sieved and separated with sieves with openings of 45 µm, 80 µm, and 120 µm.

2. EXPERIMENTAL PART

Water-atomized copper powder (supplied by Centrochem) with an irregular particle shape and electrolytic copper powder (supplied by Pometon) with a dendritic particle shape were used as starting materials. Commercial powders were sieved to obtain fractions with a narrow powder particle size distribution (in the range of about 40 µm). The powders were sieved on sieves with openings of 45 µm, 80 µm, and 120 µm. In this way, three fractions were obtained: - 45 µm, + 45 µm - 80 µm, and + 80 µm - 120 µm. The powder's designations are given in Table 1. The first letter in the designations indicates whether the powder was obtained by water-atomization (A) or by electrolytic method (E). Other letters indicate the range of particle sizes in that powder: very fine (VF) with particles below 45 µm, fine (F) with particles from 45 µm to 80 µm, and medium (M) with particles from 80 µm to 120 µm. This classification is based on the paper [7].

Table 1. The powder's/sample's designation

Fractions	Atomized powders	Electrolytic powders
- 45	A-VF (Atomized - Very Fine)	E-VF (Electrolytic - Very Fine)
+ 45-80	A-F (Atomized - Fine)	E-F (Electrolytic - Fine)
+ 80-120	A-M (Atomized - Medium)	E-M (Electrolytic - Medium)

The characterization of the powders included the determination of the shape and morphology of the particles, particle size distribution of powders, the apparent density, and the flow rate of the powders. The shape and morphology of the particles were determined using SEM "Tescan VEGA 3LMU" microscope. The average particle size and particle size distribution of each powder were obtained based on SEM microphotographs, using the image analysis software ImageJ. The particle size was measured along the longest axis. The apparent density and the flow rate of the powders were examined using the Hall flowmeter funnel. The apparent density was done according to the ISO 3923 standard, and the flow rate was determined according to the ISO 4490 standard [8, 9].

The powders were further compacted on a hydraulic press "Mohr & Federhaff & Losenhausen" with a pressure of 600 MPa. The compacts were sintered in a furnace "Elektron ELP-08" in an atmosphere of argon at a temperature of 1000 °C for 2 h, to obtain sintered parts. Density, hardness, and electrical conductivity were measured and the microstructure was analyzed using optical microscopy. The hardness was measured using "VEB Leipzig" Vickers hardness tester with a load of 10 kg. The device "Institute dr. Forster Sigmatest 2.063" was used for measuring electrical conductivity. The optical microscope used to observe the microstructures was "Carl Zeiss Jena Epytip 2".

3. RESULTS AND DISCUSSION

3.1 Characterization of powders

Figure 1 presents SEM microphotographs of copper powders with different sizes and shapes depending on the obtaining method. The water-atomized powders (Figs. 1a-1c) appear in an irregular shape while the electrolytic powders show a typical dendritic shape (Figs. 1d-1f).

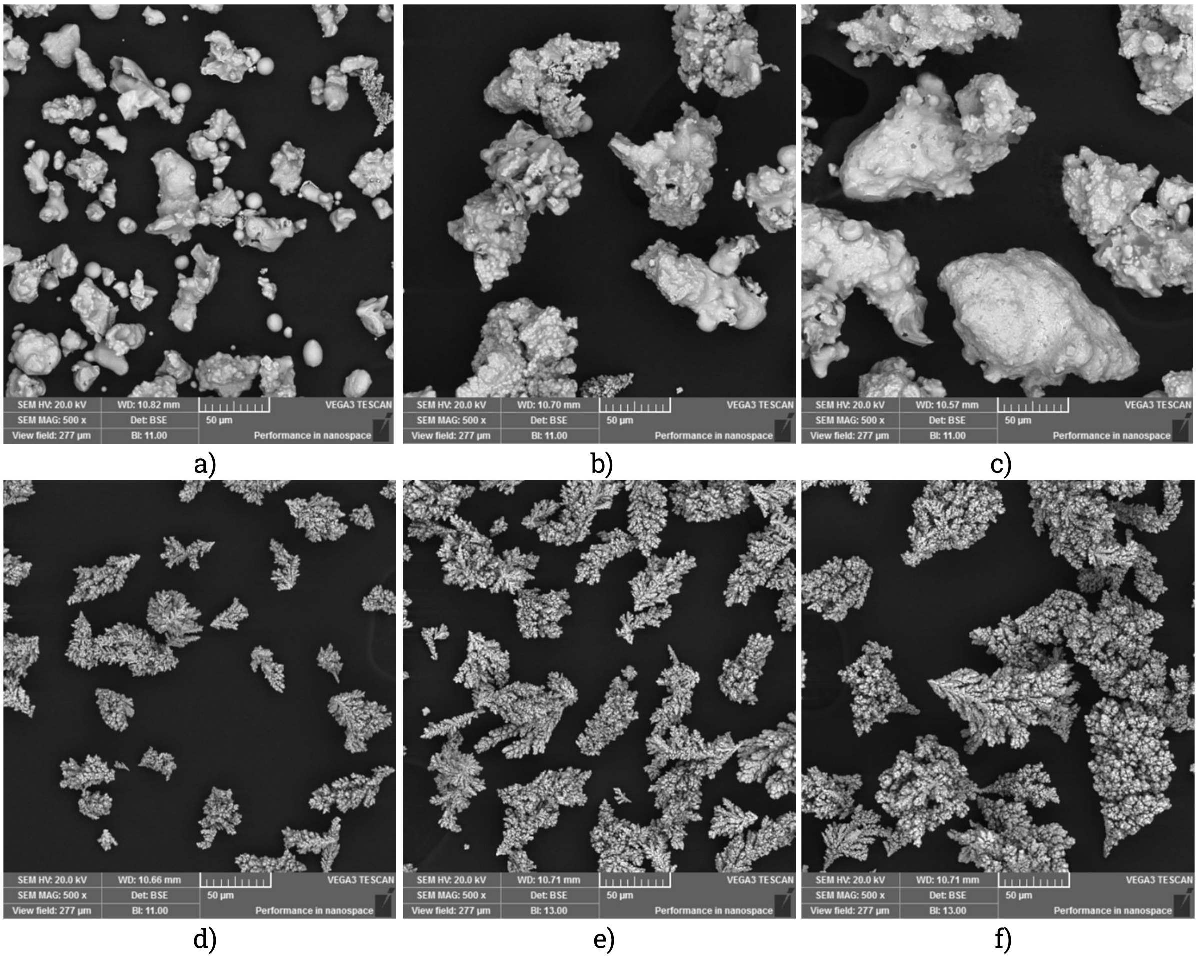
a) b) c) d) e) f)

Figure 1. SEM microphotographs of copper powders (a) A-VF; (b) A-F; (c) A-M; (d) E-VF; (e) E-F; (f) E-M

Figure 2 shows the average particle size and particle size distribution of atomized copper powders A-VF, A-F, and A-M. The A-VF powder has the finest average particle size as compared to others, which is 25.2 µm. Powder A-F is coarser, with an average particle size of 64.7 µm. The powder A-M is the coarsest with an average particle size of 125.7 µm.

Figure 3 shows the average particle size and particle size distribution of electrolytic copper powders E-VF, E-F, and E-M. The E-VF powder has the finest average particle size, which is 36.4 µm. Powder E-F is coarser, with an average particle size of 51.7 µm. The coarsest electrolytic copper is E-M powder with an average particle size of 84.2 µm.

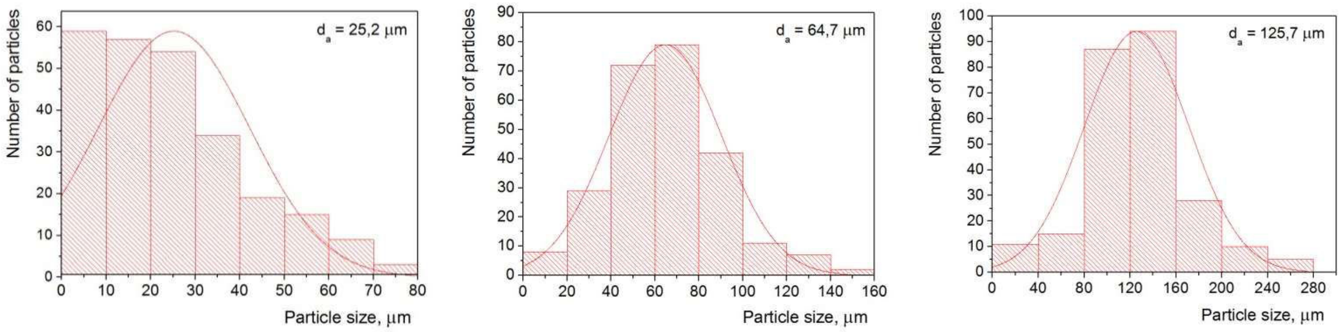

a) b) c)

Figure 2. The average particle size (d_a) and particle size distribution of atomized copper powders (a) A-VF; (b) A-F; (c) A-M

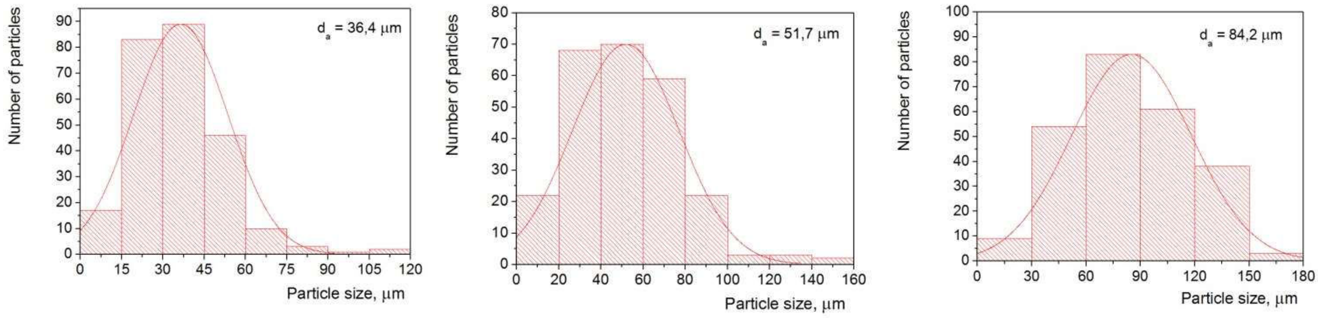

a) b) c)

Figure 3. The average particle size (d_a) and particle size distribution of electrolytic copper powders (a) E-VF; (b) E-F; (c) E-M

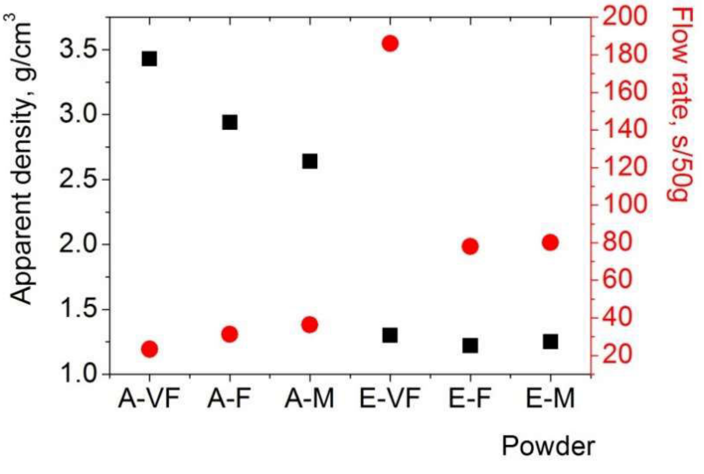

Figure 4. The apparent density and the flow rate of loose powders

Comparing the same fractions of atomized and electrolytic powder, it can be noticed that VF atomized powder is finer than electrolytic one, while F and M atomized powders are coarser than F and M electrolytic copper powders, respectively.

Figure 4 shows the apparent density and the flow rate of loose powders. The apparent density of the metal powder is influenced by the theoretical density of the metal, the granulometric composition of the powder, particle shape, surface and roughness of the individual particles, particle packing, oxidation degree, and porosity. Generally, the apparent density increases with an increase in particle size (this behavior was not shown in this paper, but vice versa), if the particle shape becomes less spherical and more irregular and with an increase in surface roughness [10].

It is generally observed that atomized copper powders have higher apparent densities and flow rates compared to electrolytic powders. This is related to the shape of the particles. In the case of dendritic electrolytic copper powder, the presence of bulges and dents in the particle surface, as well as the increase in the specific surface area of the particles increase the friction between particles, this makes it difficult to move the particles relative to each other and causes poor packing of the dendrite particles. Because of that, atomized powders have a higher apparent density and flow rate than dendritic powders [11, 12]. The highest apparent density and flow rate are observed for A-VF powder (3.43 g/cm^3 and 23.32 s/50g, respectively). The lowest apparent density was achieved in E-F powder (only 1.22 g/cm^3), while E-VF powder showed the lowest flow rate (186 s/50g).

3.2 Characterization of sintered parts

Figure 5 shows the results of measuring the densities of green compacts and sintered parts from different types of powders. It can be concluded that the density of sintered parts decreased compared to the density of green compacts. This is unusual behavior. The expansion of the parts most likely occurred due to the reaction of residual gases in compacts with the atmosphere in the sintering furnace, i.e. with residual oxygen inside the furnace.

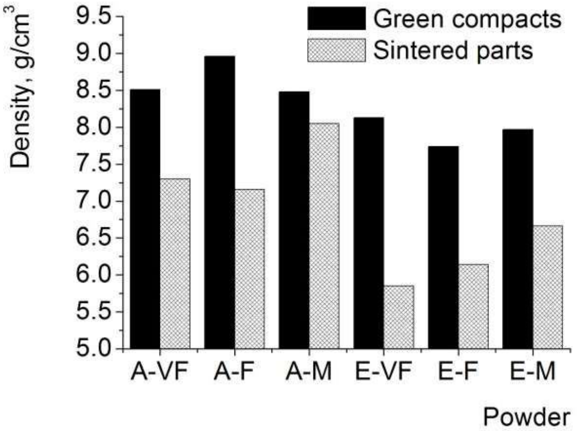

Figure 5. The densities of green compacts and sintered parts

Sintered parts obtained from atomized copper powders have significantly higher density values compared to parts obtained from electrolytic copper powders. In the case of parts obtained from electrolytic copper powder, a clear tendency is observed that the density of the parts increases with an increase in the particle size of the starting powder. The same results were obtained by Chang and Wu [4]. This tendency is not expressed in parts obtained from atomized copper powder.

Figure 6 shows the microstructures of sintered parts obtained from atomized powders with different particle sizes. Polygonal grains with annealing twins are observed. The tendency of grains and microstructure consolidation is observed with an increase in the particle size of the starting powder from which the parts were obtained. Spherical pores are present at the grain boundaries and within the crystal grains themselves. The porosity is indicated, especially for the samples obtained from powders A-VF and A-M.

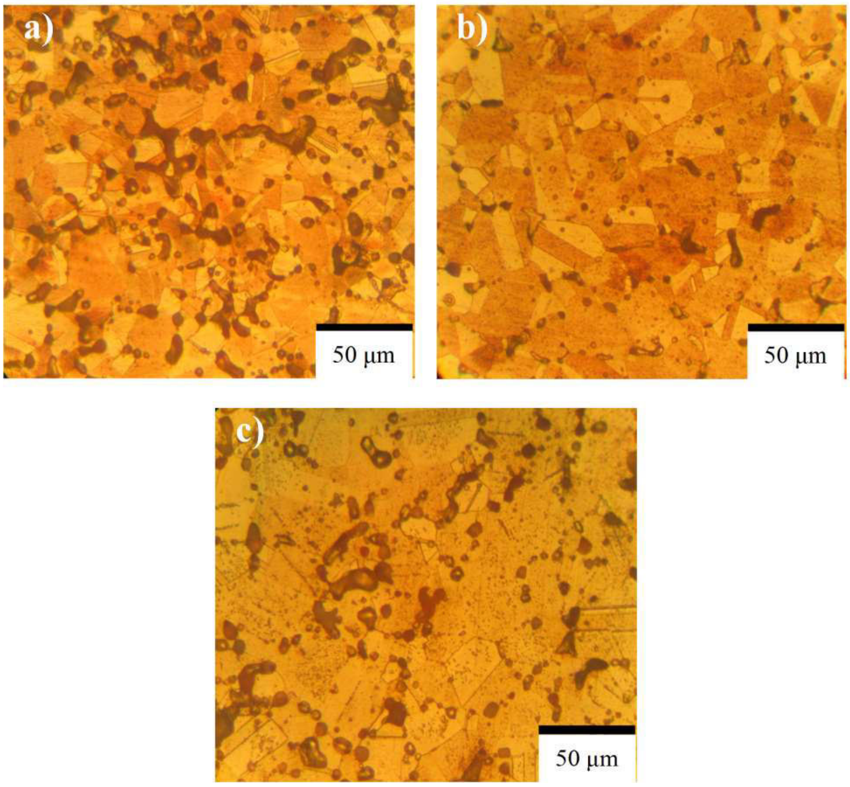

Figure 6. Optical micrographs of sintered copper obtained from atomized powder (a) A-VF; (b) A-F; (c) A-M

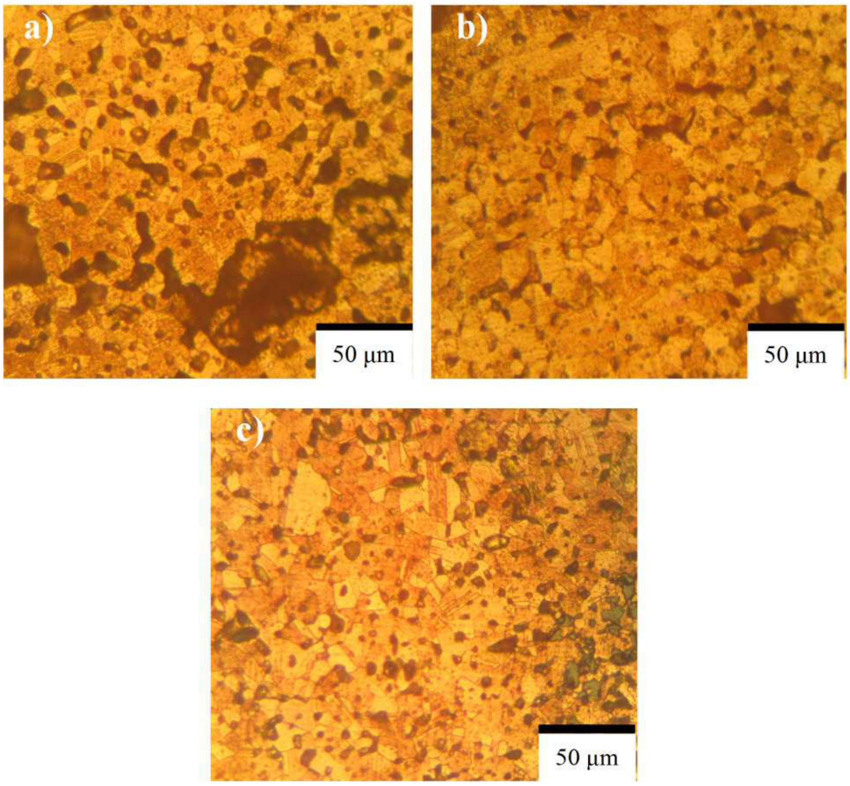

Figure 7. Optical micrographs of sintered copper obtained from electrolytic powder (a) E-VF; (b) E-F; (c) E-M

Figure 7 presents the microstructures of sintered samples obtained from electrolytic powders with different particle sizes. For the same starting powders (the same fractions), a finer-grained microstructure was observed in parts obtained from electrolytic powders compared to parts obtained from atomized powders. The microstructure is dominated by pores, which are large and different in shape. All sintered parts are more porous compared to samples obtained from atomized copper powders. The porosity is the most pronounced for the sample obtained from the electrolytic E-VF powder with the finest particle size, which was also confirmed by the results of the density measurement.

Figure 8 shows the hardness and electrical conductivity of sintered parts obtained from powders of different sizes and shapes. Sintered parts obtained from atomized powders have higher hardness and electrical conductivity values compared to parts obtained from electrolytic copper powders. This is understandable, considering the higher density values of the parts obtained from atomized copper. The sample from A-M powder has the highest hardness value, which is 34.57 HV10. The sample from A-F powder has the highest electrical conductivity, which is 38.15 MS/m. The lowest values of hardness and electrical conductivity were obtained for the parts obtained from the electrolytic copper powder E-VF with the finest particles, which also showed the lowest density value.

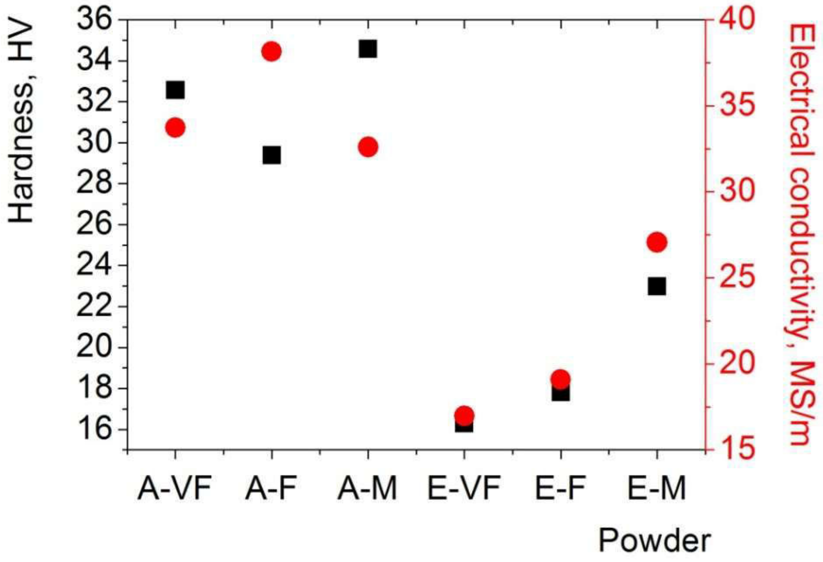

Figure 8. Hardness and electrical conductivity values of the sintered parts

4. CONCLUSIONS

The influence of the copper particle shape and size on some properties of powders, compacts, and PM parts was analyzed. The following conclusions can be drawn:

- Atomized powders showed higher values of apparent density and flow rate compared to electrolytic powders. Increasing the particle size of atomized powder showed a decrease in apparent density and flow rate (atypical behavior). However, increasing the particle size of electrolytic powder showed an increase in flow rate (typical behavior).
- The density of the sintered parts decreased compared to the density of the compacts. Sintered parts obtained from atomized powders have significantly higher density values compared to parts obtained from electrolytic powders.
- The finer microstructure was achieved in sintered parts obtained from electrolytic powders but with much more pronounced pores compared to

the parts obtained from atomized powders.

- Sintered parts obtained from atomized powders have higher hardness and electrical conductivity values compared to parts obtained from electrolytic powders.

Acknowledgement

The research presented in this paper was done with the financial support of the Ministry of Science, Technological Development and Innovations of the Republic of Serbia, with the funding of the scientific research work at the University of Belgrade, Technical Faculty in Bor, according to the contract with registration number 451-03-47/2023-01/200131.

Conflicts of Interest

The authors declare no conflict of interest.

5. References

[1] O. D. Neikov, S. S. Naboychenko, *Handbook of Non-Ferrous Metal Powders: Technologies and Applications*, Elsevier, Netherlands, 2009

[2] M. Delavari, A. Salarvand, A. Rahi, F. Shahri, The Effect of Powder Metallurgy Process Parameters on Mechanical Properties of Micro and Nano-Iron Powder, *IJEST, 3*(2011) 9, p. 86-94

[3] N. Kumar, A. Bharti, M. Dixit, A. Nigam, Effect of Powder Metallurgy Process and its Parameters on the Mechanical and Electrical Properties of Copper-Based Materials: Literature Review, *Powder Metall. Met. Ceram.,* 59(2020) 7-8, p. 401-410

[4] C. C. Chang, M. R. Wu, Effects of Particle Shape and Temperature on Compaction of Copper Powder at Micro Scale, *MATEC Web of Conferences*, 123(2017) 00011

[5] O. O. Edosa, F. K. Tekweme, K. Gupta, A Review on the Influence of Process Parameters on Powder Metallurgy Parts, *Eng. Appl. Sci. Res.*, 49(2022) 3, p. 433-443

[6] F. Sanchez, A. M. Bolarinl, P. Molera, J. E. Mendoza, M. Ocampo, Relationship Between Particle Size and Manufacturing Processing and Sintered Characteristics of Iron Powders, *Rev. Latinoam. de Metal. y Mater.*, 21(2003) 1, p. 6

[7] N. Vlachos, I. T. H. Chang, Investigation of Flow Properties of Metal Powders from Narrow Particle Size Distribution to Polydisperse Mixtures Through an Improved Hall-Flowmeter, *Powder Technol.*, 205(2011) 1-3, p. 71-80

[8] International Standards Office, *ISO 3923-1:2008, Metallic Powders - Determination of Apparent Density - Part 1: Funnel Method*, Geneva: ISO. 2008

[9] International Standards Office*, ISO 4490:2018, Metallic Powders - Determination of Flow Rate by Means of a Calibrated Funnel (Hall Flowmeter),* Geneva: ISO. 2018

[10] I. Yadroitsev, Selective Laser Melting, *Direct Manufacturing of 3D-Objects by Selective Laser Melting of Metal Powders*, LAP Lambert Academic Publishing, 2009

[11] F. Thummler, R. Oberacker, *An Introduction to Powder Metallurgy*, The Institute of Materials, London, UK, 1993

[12] I. Uslan, Y. Usta, S. Saritas, The Effects of Powder Morphology on the Apparent Density and the Flow Rate of Metal Powders, *Powder Metallurgy World Congress & Exhibition* (PM 2006), Held in Busan, Korea, September 24-28, 2006

JST&M 4(2023), 30 - 35
DOI: 10.57131/jstm.2023.4.5

Professional paper

EFFECT OF ADDITION OF WET-STRENGTH AGENT ON TENSILE STRENGTH OF PAPER

Edina Husić[1], Šefkija Botonjić

[1]Natron-Hayat d.o.o. Maglaj,

ABSTRACT

Wet-strength paper production is of great significance due to its prominent importance in everyday consumer activities. Recently, market demands for paper with specific properties and purposes are increasing. Production of these paper types is very challenging for the manufacturer since they have to meet very specific demands. Wet-strength paper products include bags that come in contact with moisture and wet products, hygienic and kitchen towels, paper towels, packaging products (packages for liquids, aseptic dishes, and a variety of packaging for food), and other special purposes items (tea bags, coffee filters, paper money, etc.) Throughout this research, the focus was on the effects a wet-strength agent has on the tensile strength of paper. The wet strength property of paper is the ratio between the strength of paper in the wet and dry state. The strength in the dry state comes from the hydrogen bonds present in natural cellulose, while the strength of paper in the wet state requires waterproof (covalent) bonds created by the use of a wet strength agent. The wet strength agent used is a cationic PAE resin. The aim of the work is to determine the optimal amount of agent needed in relation to the required value of the tensile strength property of the paper. The investigation of these influences was carried out on Semi Extensible Standard Kraft type of paper in Natron-Hayat.

Keywords: paper, wet strength additive, tensile strength

Corresponding Author:
Edina Husić
Natron-Hayat d.o.o., Lijesnica/Maglaj, B&H
Tel: +387 32 601 180
E-mail address: edina.husic@natron-hayat.ba

1. INTRODUCTION

Wet strength paper is paper that holds a significant portion of its original strength (strength in the dry state) after being completely saturated with an aqueous solution. In order to produce this type of paper, which needs to maintain its strength after being made and in a wet state, chemical agents are used. Wet-strength chemicals such as UF-urea formaldehyde, MF-melamine formaldehyde, PAE-polyaminoamide epichlorohydrin, and others are used to develop and maintain the mechanical strength of paper when the paper comes in contact with moisture. According to the chemical composition of these agents, they act either as protective agents by preventing fiber swelling and protecting existing bonds or form new and waterproof bonds through reinforcement mechanisms. In order for the paper to be used for the production of bags, it needs to have extremely good physical and mechanical properties, both in the longitudinal and transverse directions [1]. The need for such high mechanical performance of paper is based on the fact that modern technologies for filling bags and transporting them require high durability of bags [2]. On the other hand, one must always look at the financial viability of the product, which means that the goal is to produce the best possible product with as little cost as possible. Thus, in order to be competitive in the market, some other subtypes of sack kraft paper have been developed from the basic offer of sack kraft paper, which has its advantages in the production of bags. The wet strength property of paper is the ratio between the strength of paper in the wet and dry state. Unlike the strength in the dry state, which comes from the hydrogen bonds present in natural cellulose, the strength of paper in the wet state requires waterproof (covalent) bonds. Naturally, cellulose contains few covalent bonds, so additives are needed that will affect the formation of these bonds. Polymer resins are most commonly used to increase the strength of wet paper. There are two different Wet strength mechanisms, the protection mechanism, and the amplification mechanism, which are shown in Figure 1 [3].

Figure 1. Representation of wet strength mechanism of action: a) protection mechanism, b) amplification mechanism [3]

The protection mechanism involves the diffusion of the wet-strength polymer to the fiber surface where it binds through and around the fibers. In this way, they prevent swelling of the fibers and help preserve covalent bonds when the paper is exposed to water. In contrast, the reinforcement mechanism means that new bonds are formed between the wet-strength polymers and the fibers. Since the dry strength of different types of paper varies according to different parameters such as weight, density, and forces between the fibers, it is difficult to determine the strength in the wet state. Therefore, the wet strength property of paper is usually represented by the ratio between the strength of the paper in the wet and dry state. When paper comes in contact with water, water molecules increase the distance between individual cellulose fibers, so that much of the strength is lost. The paper strength is then only about 10% of the dry strength. This percentage is usually considered to represent the friction force between the residual pulp forces [4].

1.1 The Basic Mechanism of Fiber Strength

The strength of the paper depends on the strength of the bond between the individual fibers, the fiber distribution, and the bond (formation).

In the paper, fibers are joined by Van der Waals bonding forces and hydrogen bonds that give the paper mechanical and essential structural strength. Figure 2 shows the hydrogen bonds within and between cellulose fibers [5].

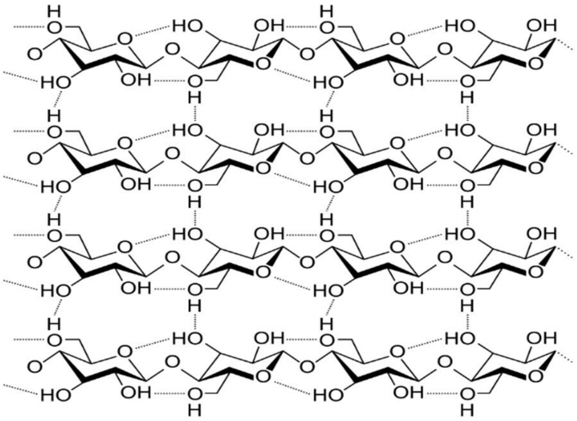

Figure 2. Cellulose fiber with hydrogen bonds (dashed lines) within and between cellulose molecules [6]

Binding affects both the development of the structure and the final structure of the paper. The bond between the fibers can be viewed as a zone in which two fibers are so close to each other that molecular entanglement or chemical bonding can occur. Bonds hold the fibers together and therefore contribute to the internal cohesion of the paper [6].

When paper is in contact with water, the hydrogen bonds between the fibers get broken. In this way, the paper loses its mechanical strength. The strength of normal paper after wetting is small, usually 4-10% of its strength when dry. Therefore, additives can be added to cellulose, chemicals for wet strength, which protect the bonds between the fibers and increase the strength of wet paper. The most commonly used agents are polymer resins [7].

2. ANALYSIS OF THE IMPACT OF "WET STRENGTH" CHEMICALS ON THE PHYSICAL AND MECHANICAL PROPERTIES OF PAPER

The influence of Wet strength chemicals on the mechanical properties of paper was investigated and the data of 33 reels (460 tons of paper) to which the chemical was added were processed. An individual analysis of each reel of paper was performed. Analysis of NH Wet Strength semi-extensible paper was performed in the internal laboratory at Natron-Hayat in Maglaj using the following methods:

- The standard method of Natron-Hayat NH F 6: Determination of tensile properties, constant load speed method (ISO 1924-1), and constant stretch speed method (ISO 1924-2 and ISO 1924-3) [8,9].
- The standard method of Natron-Hayat NH F 21: Determination of tensile strength after immersion in water [10].

The addition of chemicals to the system was done gradually from a larger amount to a smaller one in order to find the optimal consumption for the required percentage of wet paper strength. The amount of chemical dosed at the pump, at the time of completion of the reel of paper was monitored, after that the paper on the given reel was analyzed according to the previously mentioned methods, and from the obtained data a comparison of the mentioned parameters was made.

Figure 3 shows the amount of added chemical and the direct impact on the property of wet strength paper (md direction of measurement) on the analyzed paper reels.

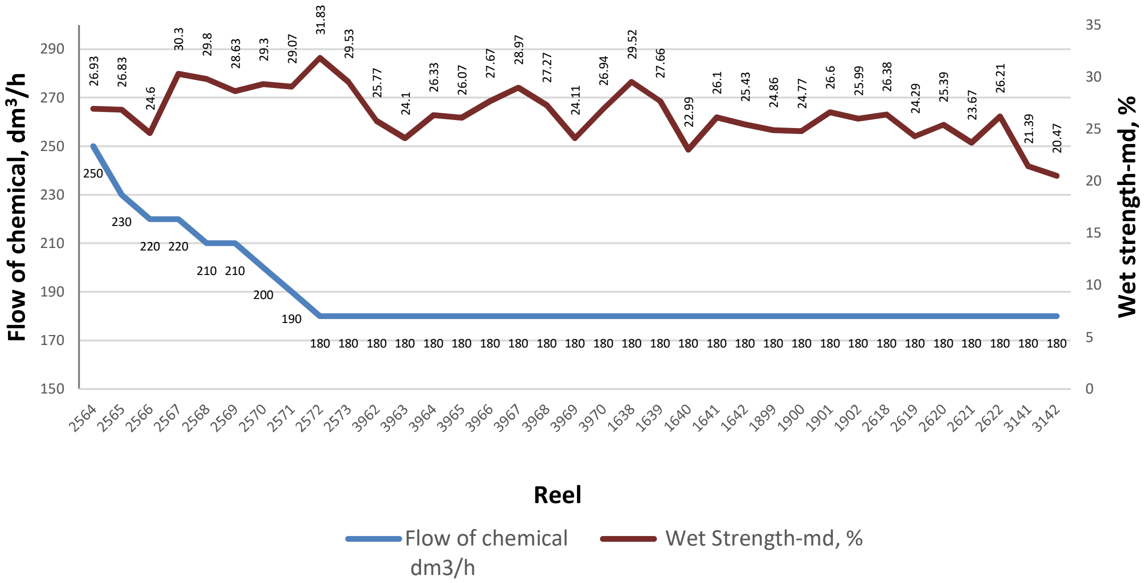

Figure 3. Effect of the addition of wet strength chemicals - md paper direction

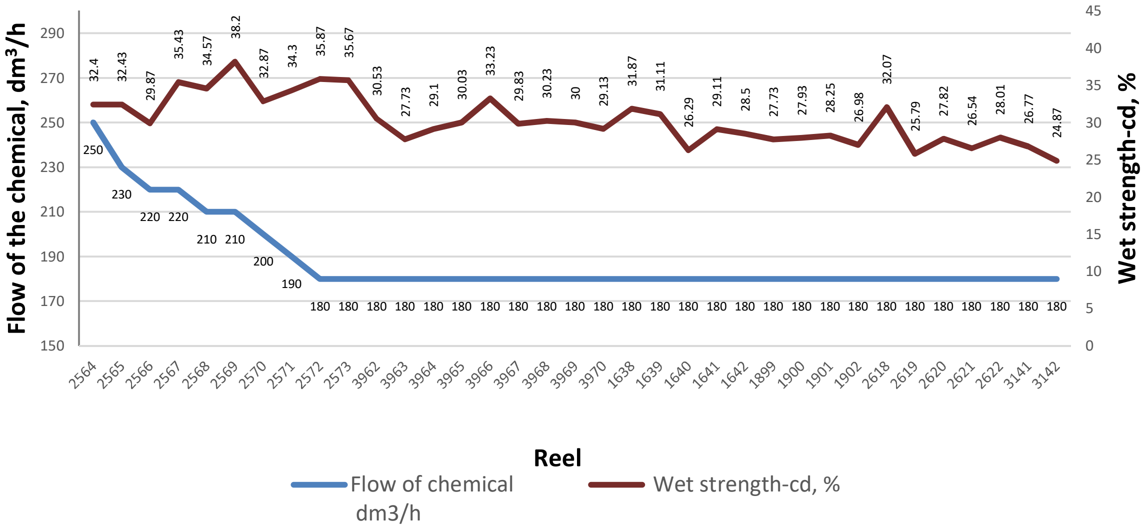

Figure 4. Effect of the addition of wet strength chemicals - cd paper direction

Figure 4 shows the amount of added chemicals and the direct impact on the property of wet strength paper (cd direction of measurement) on the analyzed paper reels.

Figures 3 and 4 show how much of an effect adding the chemical has on the wet strength of paper in the machine direction and cross direction. From the presented results the optimal amount of chemical consumption that meets the required wet strength value can be seen. Due to the need to saturate the system, a larger amount of agents was added at the beginning. The measured values of wet strength (in the cd and md direction) were lower on the first analyzed tambourines because it is necessary to saturate the system with the added wet strength additive. Then, smaller amounts of the agent were added and higher values of the wet strength cd and md properties were obtained on the following reels. In order to find the optimal ratio of the amount of added agent and the required value of wet strength, the amount was reduced to 180 dm3/h or 5 kg/t of paper, whereby the required wet strength value was obtained.

In order to have an insight into the influence of chemicals on the physical and mechanical properties of paper, the analysis of semi-extensible paper without the addition of wet-strength chemicals was performed. Figure 5 compares the values of tensile strength, measured in the MD and CD directions of the paper, in the dry and wet state in the case when no wet Strength chemical was used during production.

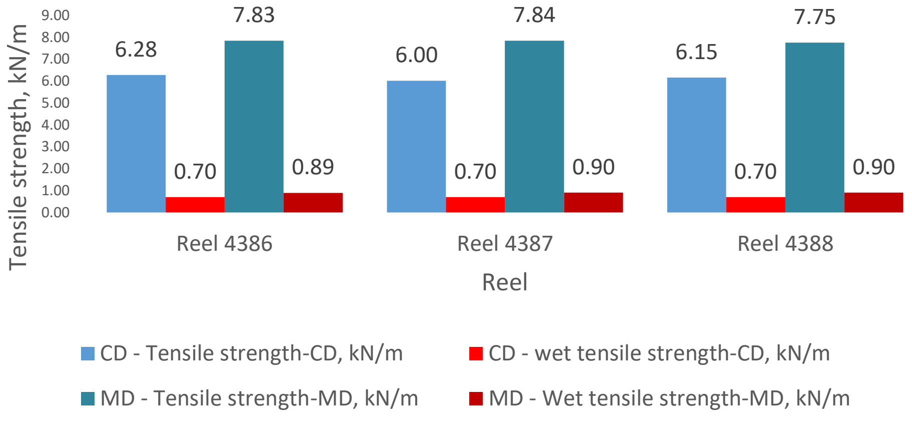

Figure 5. Tensile strength in dry and wet state in cd and md direction

Figure 5 shows the measured value of tensile strength in the dry and wet state in two directions of the paper to which no chemicals for wet strength were added. The same analysis was performed on three paper reels (42t paper). The diagram shows that the value of tensile strength in the wet state decreases sharply compared to the value of tensile strength in the dry state. On Figure 5, it can be seen that the mechanical properties of the paper in the dry state are at a high level, but after immersion in water, these values decrease. The reason for the high values of mechanical properties in the dry state for this type of paper is related to the raw material from which it is obtained, long cellulose fibers and their processing by grinding processes, and also with the help of machine orientation. The obtained values of the comparison of tensile strength in the wet and dry states shown in Figure 5 show that there is a decrease in the value by about 90% when the paper is in the wet state.

3. CONCLUSION

In this paper, theoretical research was conducted on the production of wet-strength paper and the mechanism of action of wet-strength chemicals. Based on the results of this research and research conducted in the laboratory and industrial conditions in the pulp and paper factory Natron - Hayat, the following conclusions were reached:

- Wet strength semi extensible paper as a paper with strong mechanical properties in the wet state is a sought-after product for all purposes in which the paper comes as packaging for products with a higher percentage of moisture;
- In order to obtain good physical and mechanical properties of paper in the wet state, the use of additional chemicals is required. In order to find the optimal consumption of the chemical, but also to meet the required value of paper strength in the wet state, it was concluded that the optimal value of consumption is 180 dm^3/h or approximately 5 kg/t of paper. The use of new chemicals in each production process further increases the cost of production itself, so the optimal balance must be found between the consumption of funds and the cost-effectiveness of the product.
- In order to prove the impact of chemicals on the product, an analysis of paper without the addition of chemicals was performed. Such a product does not have the strength in the wet state that is needed. By saturating the paper with water, the paper loses its physical and mechanical properties, which is proven by the analyzes in this paper. Chemicals for wet strength are those that lead to the creation of new bonds with fibers and the preservation of physical and mechanical properties when the paper is wet. Analyzes showed that the value of wet paper strength in paper to which wet strength chemicals were not added was 10%, while in paper with the addition of wet strength chemicals, depending on the amount added, this value is 20-35%;
- The impact of the amount of chemicals, i.e. the amount of chemicals consumed in relation to paper production was investigated in this paper and the results were obtained on the optimal amount of consumption per ton of paper, following the internal standard on physical and mechanical properties of paper and economic aspect;
- In order to be competitive with the market, paper mills must follow new trends in production and have papers for specific purposes in their product portfolio, such as wet strength paper.

Conflicts of Interest

The authors declare no conflict of interest

4. References

[1] Š. Botonjić, Proizvodnja celuloze i papira-teorija i praksa, Fojnica, 2017.

[2] H. Duraković, Proizvodnja clupak papira, Fojnica, 2010.

[3] H.H. Espy, *The mechanism of wet strength development in paper*, *Tappi J.* 78(1995) 4, p. 90-99

[4] L. L. Chan, *Wet-Strength Resins and Their Applications*, TAPPI Press, Atlanta, 1994

[5] C. J. Biermann, *Handbook of Pulping and Papermaking*, 2nd Edition, Academic Press Limited, London, 1996

[6] E. Husić, *Wet strength papir, hemizam i uticaj na fizičko-mehaničke osobine papira*, [Magistarski rad], Univerzitet u Zenici, Metalurško-tehnološki fakultet, Zenica, 2021.

[7] C. S. Maxwell, *Wet Strength in Paper and Paperboard*, Monograph No. 29, (J. P. Weidner, Ed.), TAPPI, Atlanta, 1965, p. 23-26

[8] International Standards Office, *ISO 1924-2:2008; Paper and board — Determination of tensile properties — Part 2: Constant rate of elongation method (20 mm/min),* Geneva: ISO.2008

[9] International Standards Office, ISO 1924-3:2005 Paper and board—Determination of tensile properties— Part 3: Constant rate of elongation method (100 mm/min), Geneva: ISO.2005

[10] International Standards Office*, ISO 3781:2011, Paper and board — Determination of tensile strength after immersion in water*, Geneva: ISO.2011

JST&M 4(2023), 36 - 48
DOI: 10.57131/jstm.2023.4.6

Review paper

POLYMERIC MATERIALS IN GLUING TECHNIQUES

Šaćira Mandal, and Aida Šapčanin

University of Sarajevo, Faculty of Pharmacy

ABSTRACT

Polymeric materials have an important role in gluing technology due to their broad application in the wood industry, metal industry, glass, and ceramics industry as well as medicine. This article discusses the basic physicochemical aspects of bonding with adhesives and also, the mechanisms of action of the adhesive materials during bonding based on polymerization processes and different types of polymerization. It was emphasized that depending on the material used in gluing, various adhesives with different physicochemical characteristics facilitate and contribute to the quality of the bonded joints. In this way, it is an insured procedure that is suitable for materials that are sensitive to the effects of heat, because welding and soldering would deform the base material and often the total degradation of its mechanical properties.

Keywords: gluing technology, adhesion, polymerization

Corresponding Author:
Šaćira Mandal,
University of Sarajevo-Faculty of Pharmacy
Zmaja od Bosne 8 (Campus), 71 000 Sarajevo, B&H
Tel. +387 33 586 189
E-mail address: sacira.mandal@ffsa.unsa.ba

1. INTRODUCTION

From time immemorial, the gluing technique has been used to make many products from different materials. Particularly successful development of bonding materials has occurred in the last two or three decades. Today, the board of gluing techniques is experiencing constant expansion due to the development of quality adhesive materials, appropriate equipment, and technological processes.

The technology of gluing is extremely important and for a long time is the dominant binding process, for example, in the wood industry, while today it is used on other basic materials such as metals, ceramics, plastics, glass, etc. Using gluing technology, especially wood as a basic material is of great use-value, and the development of new adhesives has significantly ensured the quality of the bonded joints. The application of adhesive technology on metallic materials is currently relevant for purposes of a lower degree of responsibility (medicine applications), although at the global level, more and more often it is used on structures of greater responsibility, for example in aviation.

The application of gluing technology is especially suitable for thin metal parts of different shapes and sizes, and the construction of complex shapes of different materials. The stress concentrations in the metal are minimal, there is no twisting and creasing. The adhesive technology is especially suitable for materials that are sensitive to the effects of heat because welding and soldering would deform the base metal and often the total degradation of its mechanical properties [1-5].

2. COUPLING MECHANISM USING ADHESIVES

Bonding materials are most often achieved by an adhesive-cohesive mechanism that is evident in several basic materials such as wood, metals, heat-resistant plastics, ceramics, etc. Adhesion is the force of attraction between surfaces of two or more of the same or different materials brought into direct contact. Adhesion forces lead to the formation of an adhesion bond which is a consequence of the migration of molecules of the base material into the adhesive and vice versa, where the bond is achieved by chemical bonding, and physical and mechanical bonding.

Chemical bonding implies the realization of one and covalent bonds between the base material and the adhesive.

Physical bonding is realized by dipole-dipole intermolecular forces, and mechanical is conditioned by mechanical contact of contact surfaces. The formation of chemical bonds is especially realized in the contact of metals, metal oxides, and hydroxides with adhesives, while intermolecular Van der Waals bonds are realized in the use of synthetic highly polymerized substances and in bonding polar materials such as wood (cellulose). Also, mechanical bonding is important in porous materials such as wood, while metal damage has almost no role. Cohesion forces are those that hold matter together, with the molecules of polar and non-polar compounds being interconnected by intermolecular and chemical bonds. The mechanical strength of the bonded joint is the total strength and consists of adhesion and cohesion strength and is influenced by a large number of influencing factors, the most important of which are the chemistry and structure of the adhesive macromolecules.

It is known that polar compounds and heterochain polymers with equal macromolecular chain lengths and chain parallelism have significantly greater cohesion than non-polar compounds in wood gluing. Cohesive bonding is realized by the action of Van der Waals forces, a typical chemical covalent bond, and often hydrogen bonds. The adhesives used for bonding are in the liquid state, and curing is a chemical process in which adhesive monomers polymerize by polymerization and polycondensation mechanisms, which are explained in more detail in the next section [6, 7].

3. PHYSICO-CHEMICAL ASPECTS OF ADHESIVE BONDING

The mechanism of action of the adhesive during bonding is based on polymerization processes. A polymer is a compound of high molecular weight, and the structure is such that it can be considered to be composed of many small equal parts (Greek *Polys* = many, and *meros* = part). The process by which polymers are formed is called polymerization.

3.1 Polymerization mechanisms

Polymers are defined by their mechanism, which can take place as in the following:

- chain-reaction,
- step-reaction,

Coordination polymerization is a special type of chain-reaction polymerization

3.1.1 Chain-reaction (Addition) polymerization mechanism

Polymerization by the chain reaction mechanism is reduced to free radical reactions or reactions in which ions participate as reactive particles. Depending on the type of initiator used, cations and anions can take over this function. The mechanism of the free radical polymerization chain reaction begins with the polymer chain growing by creating free radicals from unsaturated monomers that are added to the growing polymer chain to be obtained.

The presence of small amounts of initiators is required for polymerization. The most commonly used initiators are peroxides. These compounds cause the formation of free radicals by binding an oxygen molecule from peroxide to one C atom of an unsaturated compound, forming an even larger radical that further adheres to the next molecule and thus advances the chain reaction. The end of the chain reaction occurs by merging two radicals, whereby the radicals are consumed and new ones are not formed. For example, the mechanism of obtaining poly(ethene) - commonly called polythene by chain polymerization of free radicals (shown in Figure 1).

Initiation or creation of free radicals begins with the use of the molecule-initiator R = R1 which is thermally unstable and by breaking into free radicals R and R1 (where R and R1 may or may not be the same) during heating; (Reactions 1-6 and Figure 2). These created radicals then react with the monomeric unit M:

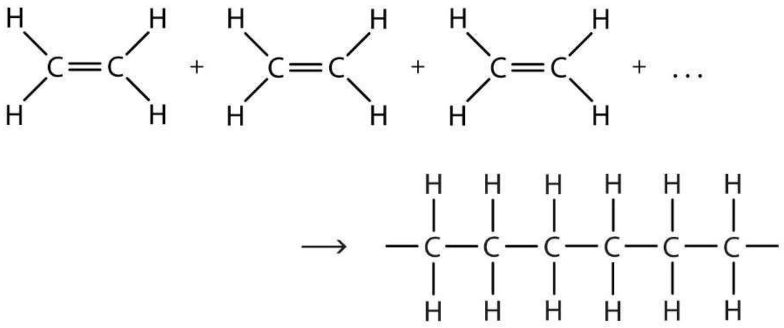

Figure 1. Chain-reaction polymerization: the reaction of a few monomer units

$$R\bullet + M \rightarrow RM \quad (1)$$

$$RM_n\bullet + RM_n\bullet \rightarrow RM_{2n}R \quad (2)$$

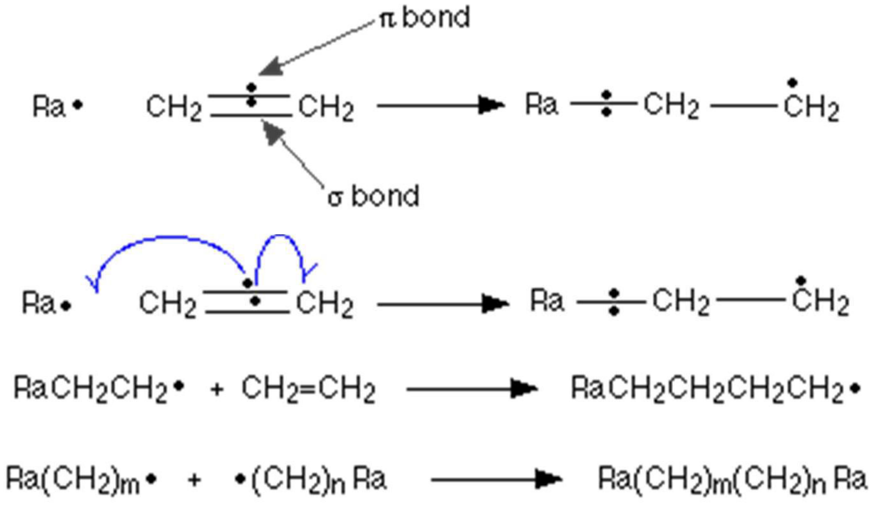

(3)

(4)

(5)

(6)

Figure 2. The reactions step of polymerization involves: (1)-initiation; (2)-propagation; (3)-termination

In the same way, the RM radical will react with the next monomer unit to form a growing polymer chain. The end of the chain and thus the reaction is formed by a combination of two radical chains that occurs at temperatures below 60 °C. The mechanism of the ionic polymerization chain reaction takes place depending on the type of compound used, so it can be cationic polymerization or anionic chain-reaction polymerization [8-12].

Cationic polymerization

Cationic polymerization takes place by a mechanism characteristic of chain reactions with the difference that the acid used here is the initiator. Different acids can be used as initiators: H_2SO_4, $AlCl_3$, and BF_3 with the addition of small amounts of water. The reaction mechanism goes through the intermediate state, which leads to the formation of carbocations (carbon ions). The formed carbocation adheres to the terminal

C-atom of the double bond and thus forms a new carbocation. This process is repeated until the chain is complete. Any of the carbon ions can be stabilized and the chain terminated by proton loss from any carbon atom located adjacent to the carbon ion. Therefore, the product always contains a double bond per polymer molecule and consists of a mixture of isomers in which, preventing further isomerization, the double bond is in positions 1, 2, or 2, 3, which can be shown as follows (Figure 3).

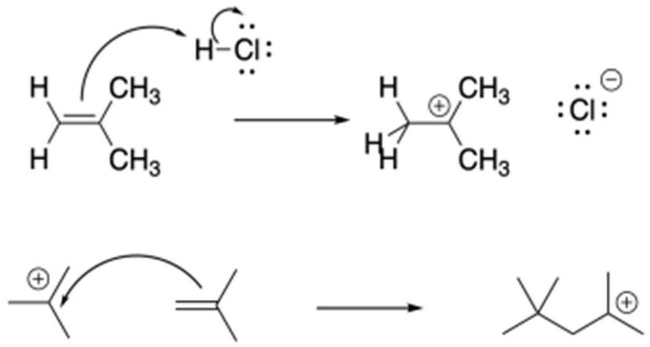

Figure 3. The cationic polymerization

An example of cationic polymerization is given for the formation of polyisobutylene and polypropylene is shown in Figure 4. Polypropylene is produced by the chain-growth polymerization of propene (Figure 5).

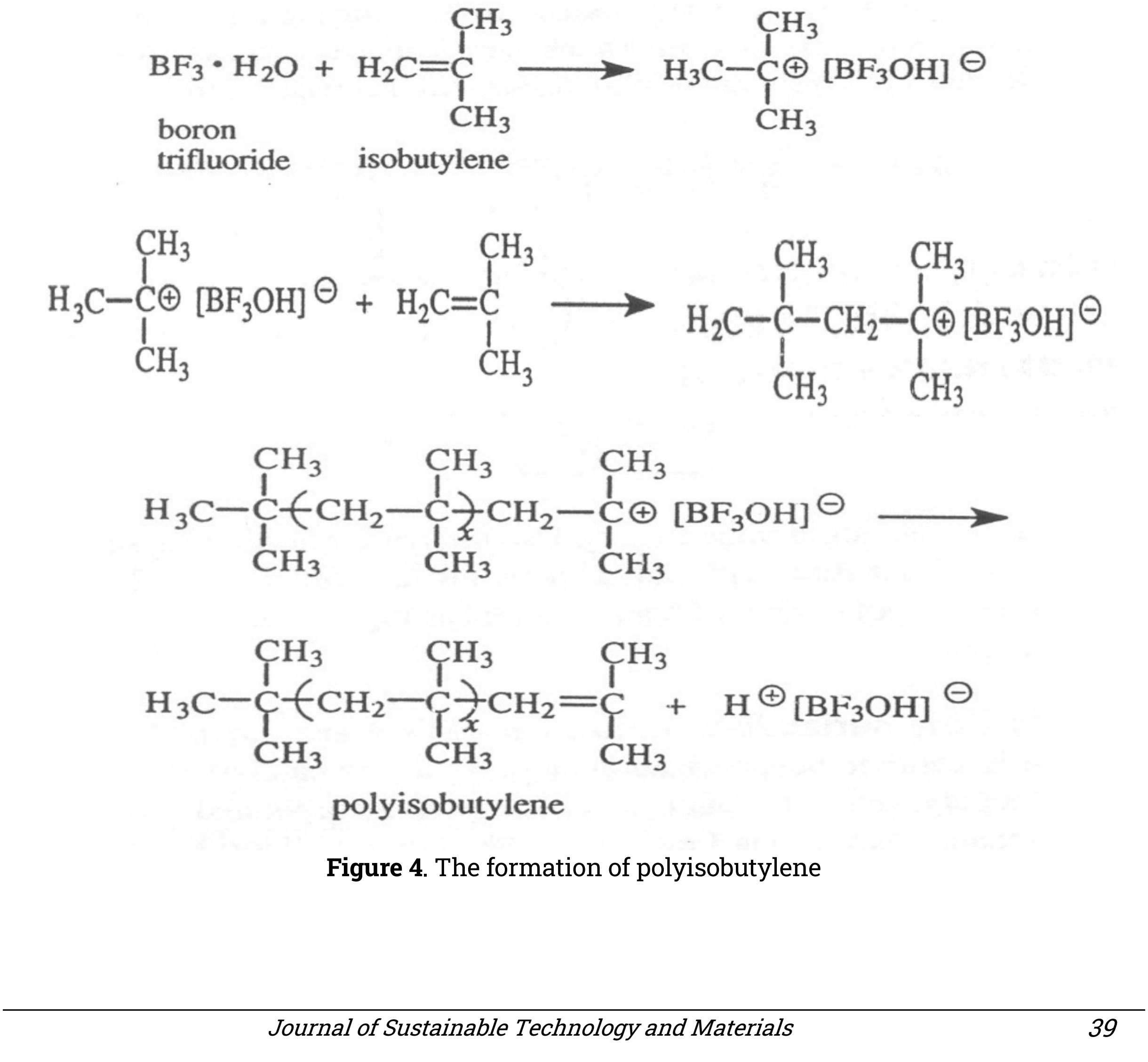

Figure 4. The formation of polyisobutylene

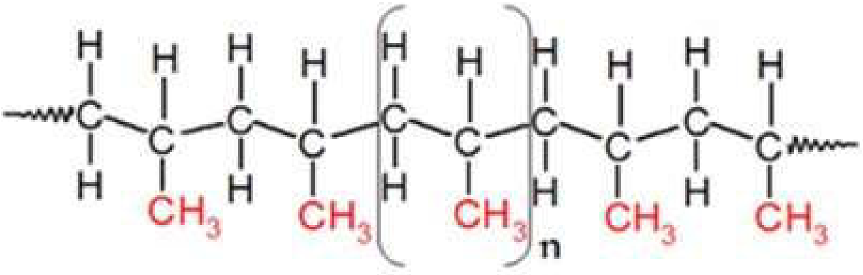

Figure 5. The molecular structure of polypropylene (PP)

Polypropylene is made from the polymerization of propene monomer (an unsaturated organic compound - chemical formula C_3H_6) by Ziegler-Natta polymerization or Metallocene catalysis polymerization (Figure 6).

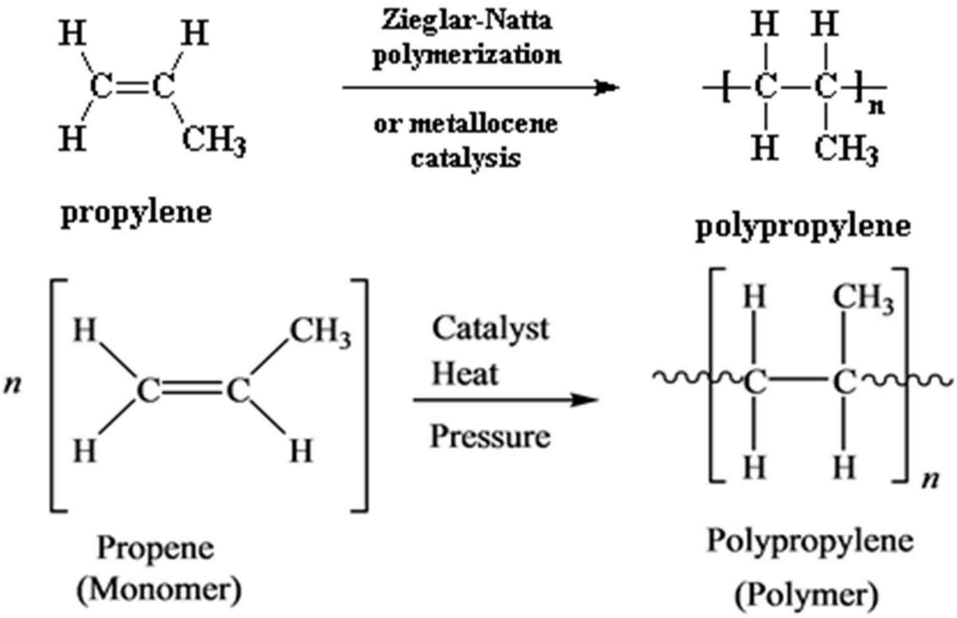

Figure 6. The formation of Polypropylene (PP)

Upon polymerization, PP can form three basic chain structures depending on the position of the methyl groups (Figure 7).

- Atactic (aPP) – Irregular methyl group ($–CH_3$) arrangement,
- Isotactic (iPP) – Methyl groups ($–CH_3$) arranged on one side of the carbon chain,
- Syndiotactic (sPP) – Alternating methyl group ($–CH_3$) arrangement

According to the used (co)polymerization or mixing process and formulation, polypropylenes can be hard or soft, opaque or transparent, light or heavy, insulating or conductive, neat or reinforced with cheap mineral fillers, short or long glass fibers, natural fibers or even self-reinforced [13-17].

Anionic polymerization

Anionic polymerization takes place by a mechanism that takes place under the influence of the anion as the initiator, i.e under the influence of a base. $LiNH_2$ in-butyl lithium is most often used as the bases that activate the molecule of the polymerizable compound, i.e. organometallic lithium compounds or some other organometallic compounds are used. A general overview of anionic polymerization is given as follows (Fig.8):

An example of this polymerization method is given for the case of polystyrene formation in Figure 9.

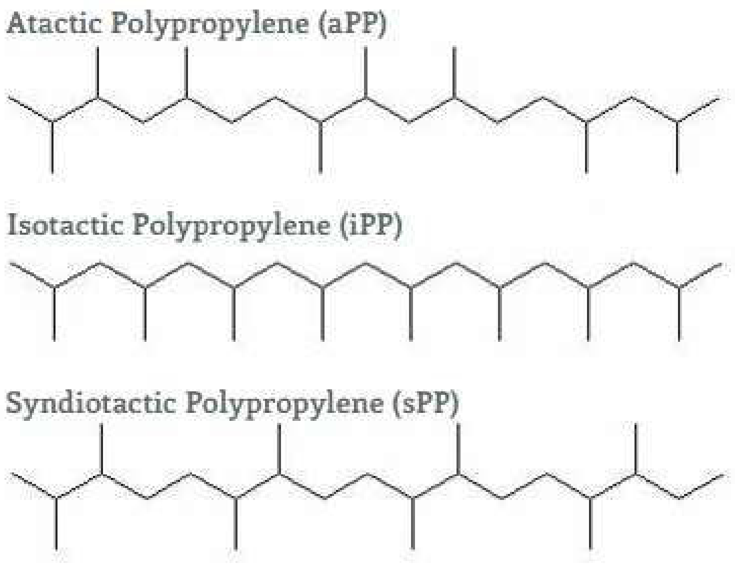
Atactic Polypropylene (aPP)
Isotactic Polypropylene (iPP)
Syndiotactic Polypropylene (sPP)

Figure 7. Basic chain structures of PP

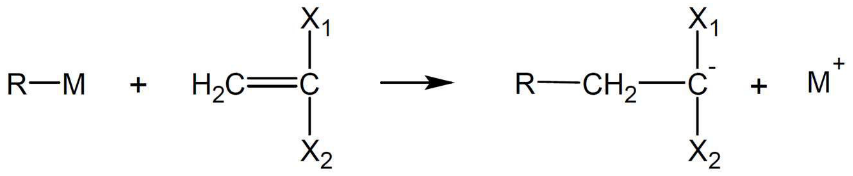

$$R{-}M + H_2C{=}C(X_1)(X_2) \longrightarrow R{-}CH_2{-}C^{-}(X_1)(X_2) + M^{+}$$

Figure 8. The anionic polymerization

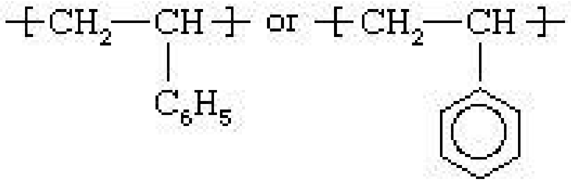

Figure 9. Basic chain structures of polystyrene

Anionic polymerization can be enhanced by the use of the metals Li and Na. For example, in the polymerization of styrene by the action of metallic Na on naphthalene, the Na atom transfers one electron (1) to naphthalene, so that the resulting radical anion gives the electron styrene (2) with the formation of styrene radical anion. Like other free radicals, the styrene radical-anion dimerizes into one dianion, which is the real initiator of this polymerization, and it begins to grow at both ends of the dianion (Figure 10).

Anionic polymerization is not limited to vinyl compounds, which react by binding to carbon-carbon double bonds. For example, the addition of a small amount of base to ethylene oxide converted into a high molecular weight polyether (Figure 11).

In anionic polymerization, the growth of the reaction chain is stopped due to contamination or the presence of a molecule that is not an integral part of the polymerization mechanism [18].

3.1.2 Coordination polymerization

In addition to the shown cationic and anionic polymerization, chain polymerization, according to the latest literature references, can also take place by a coordination mechanism. Coordinative polymerization is based on the use of metal cations and the creation of a coordination bond with organic ions [9].

industries

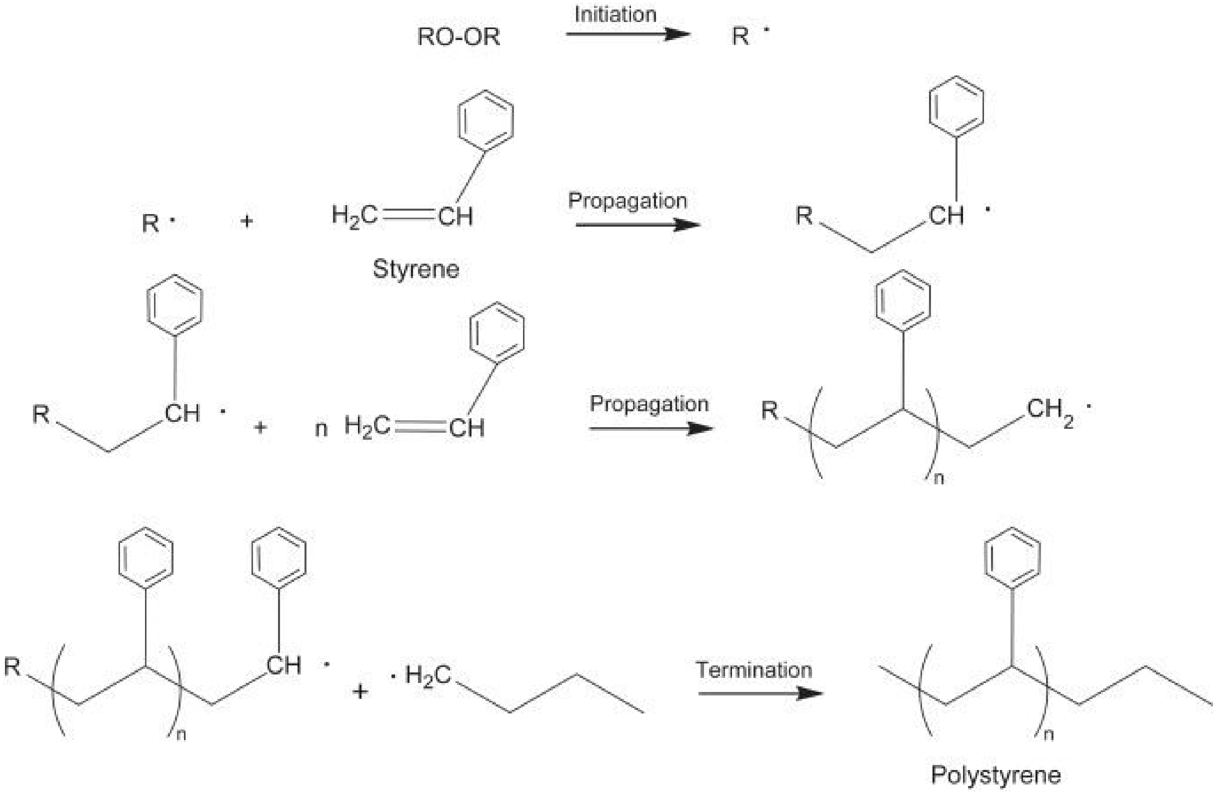

Figure 10. Polymerization of styrene

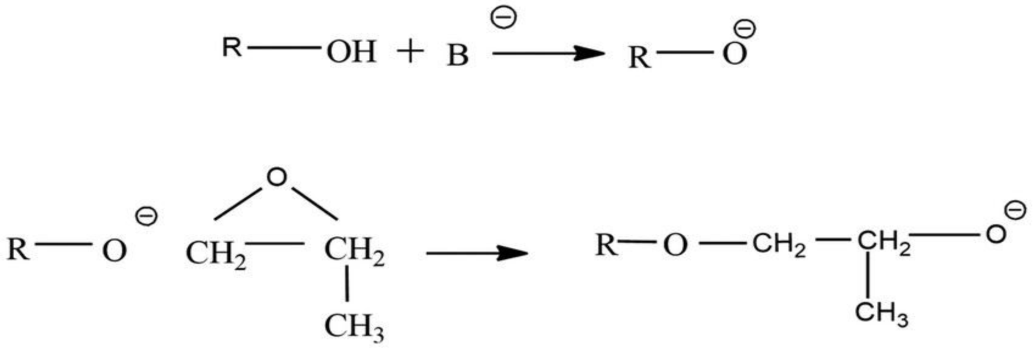

Figure 11. Basic chain structures of polyether

The introduction of ionic polymerization, and especially coordinate polymerization, has improved this area of chemistry. Particularly important here are the researches of Karl Ziegler and Giulio Natta (Nobel Prize in 1963 for work on catalysts by which the polymerization process could be controlled to such an extent as never before). These Ziegler-Natta catalysts are complexes of transition metal halides and organometallic compounds, such as triethylaluminum titanium trichloride. The reaction proceeds via nucleophilic addition to the carbon-carbon monomer double bond, with one organic group of the carbanion-like organometallic compound taking on the role of the nucleophile. The transition metal may additionally form a complex with the π-electrons of the monomer, the monomer being tightly bound at the reaction site; polymerization occurs by incorporating an alkene molecule into the bond between the metal and the growing alkyl group [10, 11].

Organic ions as chain carriers have a charge that is equal to the ion of the opposite charge or counters ion. Thus, the metal cation Li+ or Na+ is tightly bound to the growing anion. Ionic pairs as well as larger groups can play a major role in polymerases. When the bond between the reaction center and the metal is predominantly covalent, we call this reaction "coordinate polymerization." The growing organic chain is not a pronounced anion but its reactivity is based on an anion-like character. An example is the formation of polyethylene by the coordination mechanism (Fig. 12).

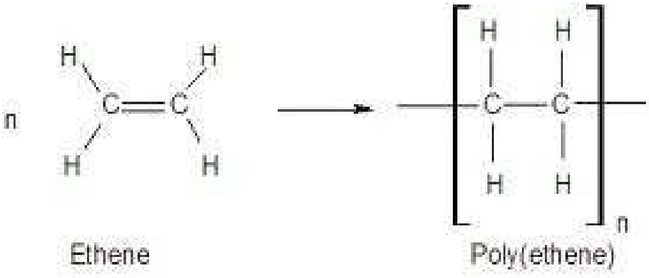

Figure 12. Polymerization of ethene

Polymerization with Ziegler-Natta catalysts has two advantages over free radical polymerization: 1) linear polymers are obtained, and 2) stereochemical control of the reaction is enabled.

For example, polyethylene, formed by free radical polymerization, has a highly branched structure, which is attributed to a special mode of chain transfer. Polyethylene, formed by coordinate polymerization (coordination process), is mostly unbranched. Unbranched molecules can easily bind to each other and then it is a polymer with a high degree of crystallinity. The exact mechanism of coordination polymerization is still unclear. However, it is believed that the transition metal is the active site. The ethylene is coordinated to the free site at the transition metal and inserted between the metal and the alkyl group R. The coordination process results in the stereospecificity of the polymerization. The rate of the reaction can be influenced by the nature of the other ligands present [13-15].

3.1.3 Step-reaction (condensation) polymerization

Polymerization by the mechanism of the stepwise reaction, i.e. polycondensation, takes place as a series of reactions that are mutually independent of each other. The polymer is formed by combining two monomer molecules into a dimer representing two molecules joined together, which can then again react with the other monomer and dimer, etc. until a long polymer is formed.

Two different functional groups are involved in the condensation polymerization reaction. These can be two different monomer particles (AA and BB) or the same monomer (AB). The reactions that take place can be illustrated by the example of the reactions that occur in the production of PET (polyethylene terephthalate) and are presented as follows:

During condensation polymerization, a water molecule or some other simple molecule or compound is separated from each newly formed bond. In the PET synthesis reaction given above (Figure 12), the alcohol combines with the carboxylic acid group to give an ester bond and water.

Another example of a condensation polymerization reaction is the synthesis and preparation of Nylon-6,6 in which a peptide bond is formed (Figure 13).

The reaction does not depend on a chain carrying free radicals or ions as in chain polymerization but the individual steps are independent of each other. If each monomer molecule contains only two functional groups, growth can only go in two directions, and a linear polymer (e.g. Nylon-6,6 or Dacron) is obtained. If the reaction can occur in more than two places on the monomer, then a highly intertwined polymer (e.g. Glyptal, alkyd resin) is formed.

In condensation polymerization, the

reactive groups at both ends of each monomer react with each other. As the chain grows, it also has reactive groups at each end so that its length can become significantly longer if the two chains join together. Condensation polymerization is used in the preparation and production of polyester, nylon, and polyurethane [19].

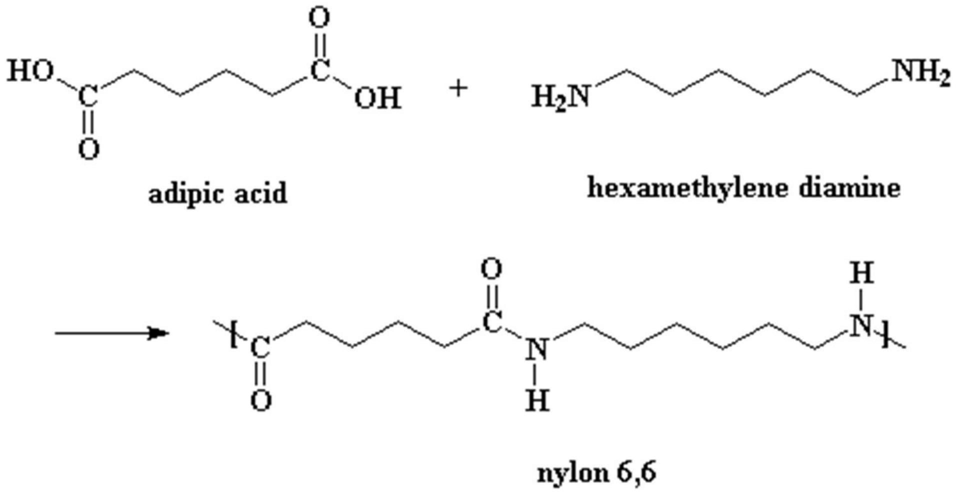

Figure 13. The condensation polymerization

4. STRUCTURE OF POLYMER/ POLYMER STRUCTURE

4.1 Microstructure

Although the fundamental property of most polymers is the degree of polymerization, the structure of the chain is a significant factor that determines the macroscopic properties of the polymer. In this sense, the terms configuration and conformation are used to describe the geometric structure of polymers. The configuration is an arrangement determined by chemical bonding. The polymer configuration cannot be changed (rearranged) until the chemical bonds are broken (broken) and rearranged. Conformation is an order that is created by rotating a molecule around a single bond. These two structures are studied further in the text [20, 21].

Configuration

There are two types of polymer configuration: *cis-* and *trans-*. These structures cannot be changed in the physical sense or by rotation. The cis configuration predominates in the molecule when substituted groups on the same side of the C = C bond (Figure 14).

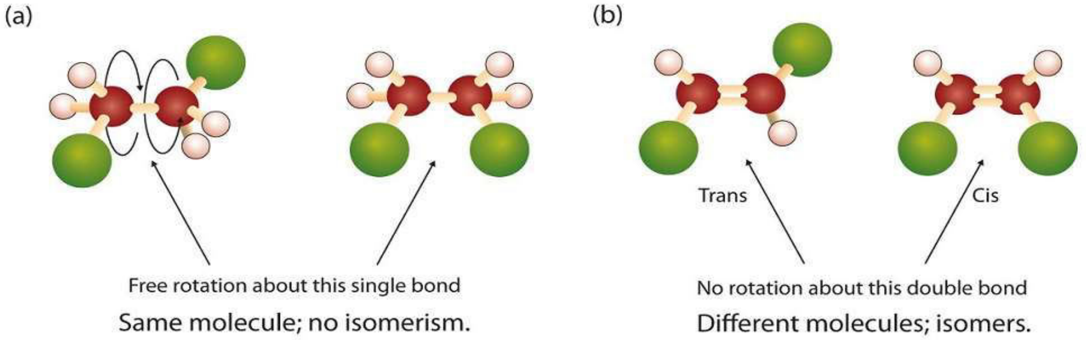
(a)
Free rotation about this single bond
Same molecule; no isomerism.
(b)
Trans
Cis
No rotation about this double bond
Different molecules; isomers.

Figure 14. The configuration of polymer

Stereochemistry (spatial arrangement) is a term used to describe the configuration of polymer chains. The three clear and distinctive structures that are obtained are called: isotactic (A), where the arrangement of all substituents is on the same side of the polymer chain; syndiotactic (B) where the polymer chain is composed of interchangeable (variable) groups and atactic (C), where the arrangement of substituents is a random or random combination of groups. The following structures show two of the three stereoisomers of the tidal chain (Figure 15). Conformation is the rotation of a part of a molecule around single bonds. If two atoms are bound by a single bond, then rotation around this bond is possible, unlike a double bond, and this does not require breaking the bond itself and results in the formation of a more energetically favorable structure.

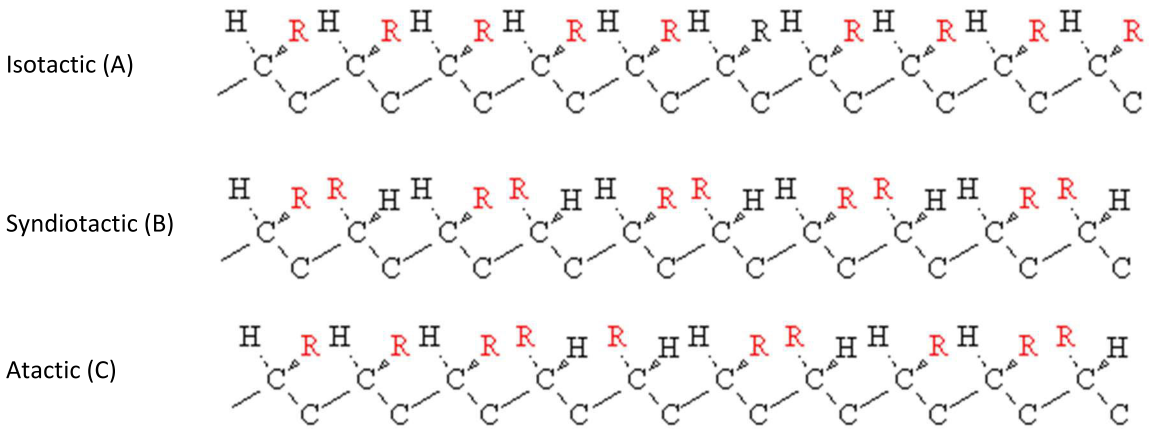

Figure 15. The configuration of polymer chains

The geometric arrangement of the bonds as a way of representing the polymer structure may vary. A branched polymer is formed when the "sides of the chain" are attached to the main chain [20, 21]. A simple example of a branched polymer is shown in Figure 16.

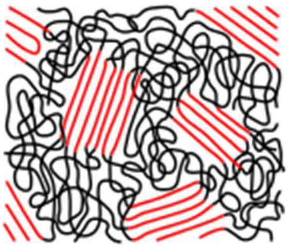

Figure 16. The configuration of a branched molecule of polymer

There are several ways to display the arrangement of branched polymers. One of these types is called "star branching". Star-shaped branching occurs when polymerization begins with only one monomer and has branches radially oriented outwards, i.e. outwards from this point. Polymers with a high degree of branching are called dendrites. Often in these molecules, the branches have their own branching. In this way, the molecules get a spherical shape in three dimensions.

4.2 Macrostructure

The shape of the molecules and how the molecules are distributed in the solid state are important factors in determining the properties of polymers. Polymers can be crystalline and amorphous. To explain the difference between crystalline and amorphous materials as well as semicrystalline, the example of glass, as an amorphous material and crystalline ice was taken. Crystalline polymeric materials show a high degree of order that is formed by assembling and accumulating polymer chains. Amorphous materials or glass-like structures show a very low degree of order and the chains are intricate, as shown in Figure 17.

In the solid-state, amorphous and crystalline materials have different heating behavior. By applying heat, the glass changes from a solid, brittle material at room temperature, to a viscous liquid in contrast, by heating, ice changes from a solid to a liquid state.

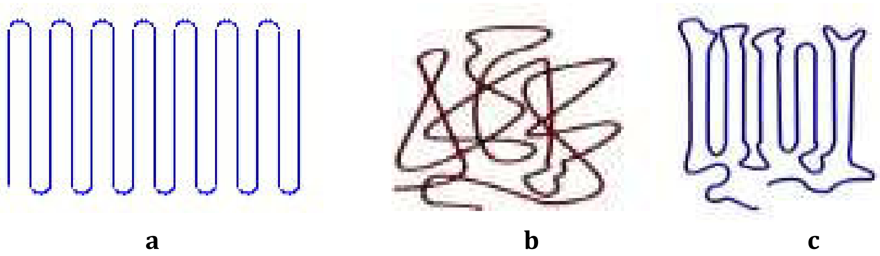

Figure 17. The arrangement of molecular chains in crystalline-**a**, amorphous-**b,** and semicrystalline-**c** polymers

The melting of the crystal leads to marked changes in the optical properties of the crystal itself. Crystalline materials have molecules arranged in repeating patterns or patterns. Salt is one of the simplest atomic structures with its components, Na and Cl ions, arranged in interchangeable arrays and the structure is cubic (cube). Salt, sugar, ice, and most metals are crystalline materials. As such, they tend to have a highly ordered and regular (symmetrical) structure [20, 21].

In contrast, amorphous materials have molecules arranged randomly in long chains that are curved and curved lines, which surround each other, thus making structures that are very different from each other. The morphology of most plumbers is a structure that is very different from each other. The morphology of most polymers is semi-crystalline, i.e. they form mixtures of small crystals and amorphous material. Some polymers are completely amorphous but most combinations with intricate and unoriented regions, surrounded by crystalline surfaces one of such combination is shown in the following Figure 18.

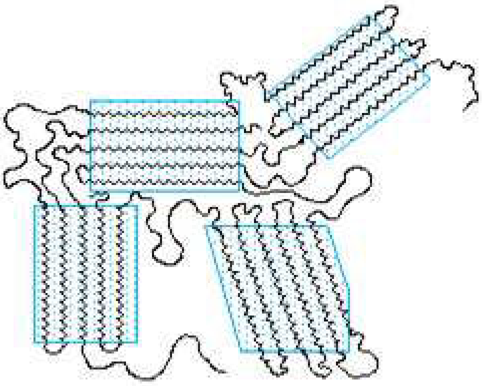

Figure 18. The morphology of plumbers

It was found that the degree of polymerization is a significant factor in determining the crystallinity of the polymer, as well as its macro mechanical properties. Polymers of lower molecular weights (short chains) are mostly crystals and generally lower mechanical strength is the reason that these are crystals and only weak Van der Waals forces act within the lattice. This allows the layers of crystals to slide slowly next to each other under tensile loads, causing the material to tear. The high degree of polymerization (amorphous polymers), on the other hand, are stronger because the molecules are in intertwined layers that are additionally connected by hydrogen bonds. In most polymers, a combination of crystalline and amorphous structures forms a material with more favorable properties in strength, i.e. in hardness and hardness. Also, the morphology of the polymer depends on the size and shape of the monomer-substituted groups. If the monomers are large and irregular, it is very difficult and complex to redistribute the polymer chain in a more orderly manner, which in turn results in an amorphous solid state. Smaller monomers and monomers that have very regular structures (like rods or rods) will form more crystalline polymers. The cooling method significantly affects the level of crystallinity. Slow cooling provides the time required for a higher level of crystallinity. Faster cooling or shorter crystallization time, on the other hand, leads to the separation of amorphous materials. Gradual curing (heating and holding at certain temperatures below the melting point of the crystal, followed by slow cooling) will lead to a significant increase in crystallinity in most polymers.

Synthetic polymers used as adhesives have different properties and they are conditioned by the chemical composition and structure of the material [22].

It has been shown that, with increasing molecular weight, the melting temperature of the polymer increases, reduces solubility, increases viscosity, and, to a certain degree, adhesion ability. Polymers that contain low molecular weight fractions to a certain extent have higher plasticity while increasing high molecular weight fractions increases strength, hardness as well as brittleness.

In the case of synthetic polymers formed by the condensation mechanism, it can generally be said that they are solid and hard. Those adhesives formed by the chain reaction mechanism melt relatively well and soften at lower temperatures.

5. CONCLUSION

The article presents the basic physicochemical aspects of bonding with adhesives. As shown, the mechanism of action of the adhesive is based on polymerization processes. In addition, the basics of adhesive polymerization by chain-reaction mechanism and step-reaction mechanism are given. Also, the mechanism of coordination polymerization, which is a special form of chain polymerization, is emphasized. This type of polymerization is important today because by using special catalysts, the polymerization process can be controlled extremely well.

Ziegler-Natta catalysts are organometallic compounds wherein the polymerization reaction takes place via nucleophilic addition to the carbon-carbon monomer double bond. By catalyzing the polymerization process, macrostructures can be achieved that provide the appropriate mechanical properties of the adhesive, i.e. the compounds achieved by their application, especially in biomedicine.

Conflicts of Interest

The authors declare no conflict of interest.

6. References

[1] N. Moszner, U. Salz, J. Zimmermann, Chemical aspects of self-etching enamel-dentin adhesives: a systematic review, *Dent Mater.*, 21(2005), p. 895-910

[2] A. Šapčanin, *Drvo-hemijski aspekt*, 1st ed., Coron's d.o.o. Sarajevo, Bosna i Hercegovina, 2019, pp. 82-100

[3] J. A. Manson and L. H. Sperling, *Polymer Blends and Composites*, New York: Plenum Press, 1976, pp. 378.

[4] L. Bateman, ed., *The Chemistry and Physics of Rubber-Like Substances*, New York: John Wiley and Sons, 1963, pp. 311.

[5] L. Pauling, R. B. Corey, H. R. Branson, The structure of proteins: two hydrogen-bonded helical configurations of the polypeptide chain, *Proceedings of the National Academy of Sciences of the United States of America 37*, 4 (1951), p. 205-11

[6] A. Pizz, and K. L. Mittal, *Handbook of Adhesive Technology*, 3rd ed., 2012, New York, NY 10016, U.S.A.

[7] C.E. Carraher, *Seymour/Carraher's Polymer Chemistry*, 7th Ed., CRC Press, Boca Raton 2008

[8] A. Ravve, *Principles of Polymer Chemistry*, 2nd ed., Kluwer Academic, New York 2012

[9] N. F. Sunday, Emerging Trends in Coordination Polymers and Metal-Organic Frameworks: Perspectives, Synthesis, Properties and Applications, *Arc Org Inorg Chem Sci.*, 1(2018), p. 39-51

[10] Giulio Natta, *J. of Poly. Sci.*, 34(1959), p. 531-549

[11] K. Ziegler, *Angew. Chem.*, 76(1964), p. 545-553

[12] W. Kaminsky, Highly active metallocene catalysts for olefin polymerization, *Journal of the Chemical Society, Dalton Transactions*, 9(1998), p. 1413-1418

[13] V. St-Onge, M. Cui, S. Rochon, J.-C. Daigle, J. P. Claverie, Reducing crystallinity in solid polymer electrolytes for lithium-metal batteries via statistical copolymerization, *Communications Materials*, 83(2021), p. 1-11

[14] F. Auriemma, C. De Rosa, A. Malafronte, M. Scoti, R. Di Girolamo, Solid-state polymorphism of isotactic and syndiotactic polypropylene, *Polypropylene Handbook*, 1(2019), p. 37-119

[15] M. D. Onofrei, A. M. Dobos, S. Ioan, Processes in cellulose derivative structures, *Nanocellulose Polymer Nanocomposites*, 1(2014), p. 355-391

[16] A. Zhugayevych, O. Mazaleva, A. Naumov, S. Tretiak, Lowest-energy crystalline polymorphs of P3HT, *The Journal of Physical Chemistry C*, 122(2018), p. 9141-9151

[17] V. Kottisch, J. O'Leary, Q. Michaudel, E. E. Stache, T. H. Lambert, B. P. Fors, Controlled cationic polymerization: single-component

initiation under ambient conditions, *J. Am. Chem. Soc.*, 141(2019), p. 10605–10609

[18] K. Ntetsikas, Y. Alzahrany, G. Polymeropoulos, P. Bilalis, Y. Gnanou, N. Hadjichristidis, Anionic polymerization of styrene and 1,3-butadiene in the presence of phosphazene superbases, *Polymers*, 9(2017), p. 1-14

[19] Naoya Ogata, Novel synthetic methods of condensation polymers and their applications as new composite and optoelectronic materials, *Pure &Appl. Chem.*, 63(1991), p. 951-960

[20] C. Hall, Polymers: molecular structure, In: *Polymer Materials*, Palgrave, London, 1981, https://doi.org/10.1007/978-1-349-10187-0_1

[21] C. De Rosa, F. Auriemma, A.Malafronte, M. Scoti, Crystal structures and polymorphism of polymers: Influence of defects and disorder, *Polymer Crystallization*, 1(2018), e10015

[22] W. F. Su, Structure morphology flow of polymer, *Principles of Polymer Design and Synthesis. Lecture Notes in Chemistry*, 82(2013), Springer, Berlin, Heidelberg. https://doi.org/10.1007/978-3-642-38730-2_3